AN INVESTIGATION INTO THE UNCONFINED COMPRESSIVE STRENGTH OF CONCRETE

by

BISWAJIT MUNSHI

B.E., University of Calcutta, 1978

A MASTER'S THESIS

submitted in partial fulfillment of the

requirements for the degree

MASTER OF SCIENCE

Department of Civil Engineering

KANSAS STATE UNIVERSITY
Manhattan, Kansas

1987

Approved by:

Major Professor

TABLE OF CONTENTS

LIST OF TABLES

LIST OF FIGURES

CHAPTER 1

INTRODUCTION AND HISTORICAL REVIEW

1.1 Introduction

Uniaxial compressive tests are the most widely accepted norm for evaluating the quality of concrete. The standard cylinder test (ASTM C39: Standard Test Method for Compressive Strength of Cylindrical Concrete Specimens (1)) is simple and provides an excellent means for the quality control of concrete in industry, and is the basis for assessing the mechanical properties of concrete which are essential to the design of concrete structures.

However, the value of ultimate compressive strength obtained from the standard uniaxial compression test, and followed religiously, is, in fact, higher than the true strength of concrete in uniaxial compression. Incorrect measurements of strength and elastic properties are obtained because of the development of non-uniform stresses throughout the specimen caused by friction between the end surfaces of the specimen and machine platens, which prevent it from expanding laterally.

Attempts have been made throughout this century to investigate the stress distribution within cylindrical specimens. Investigators have also studied the effect of specimen geometry and end conditions on the "uniaxial" compressive strength. However, a practical approach to the problem of trying to find a thumb-rule or guideline relating the strength obtained in the standard test to the true strength in unconfined compression is yet to be established. The following historical review traces significant experimental and theoretical work

in this area.

1.2 Historical Review

The effect of different end conditions on compressive strength was recognised as early as 1900 by Foeppl (2). He conducted experiments in which he eliminated end friction to a degree, and observed the modes of failure. His experiments on cubes showed that specimens with paraffin on the bearing surfaces failed at a lower ultimate strength than those without. The modes of failure were entirely different. The former failed by splitting in a direction parallel to a vertical face, whereas the latter failed in a pyramidal shape.

It was not until 1924 that Gonnerman (3) made an extensive study of this problem. He studied the influence of uneven end surfaces and of different methods of capping on the strength in compression of concrete cylinders from four different mixtures. He used neat cement paste, mixtures of gypsum and portland cement, gypsum, and a variety of other interfacing materials, such as beaverboard, white pine, millboard, leather, sheet lead, cork, and sheet rubber. He observed that the introduction of rubber sheets resulted in the greatest reduction in apparent strength -- 50 percent for a 1:3-1/2 concrete.

In the following year, Gonnerman (4) conducted a study on the effect of size and shape of test specimen on compressive strength. Cylinders 1-1/2 in. to 10 in. in diameter and two diameters in length, 12 in. in length ranging from 3 in. to 10 in. in diameter, 6 in. in diameter ranging from 3 to 24 in. in length, cubes 6 and 8 in., and square prisms 6 by 12 in. and 8 by 16 in. were tested at ages from 7

days to 1 year. A decrease in strength ratios of 5 percent and 10 percent in cylinders of height-to-diameter ratios of 3.0 and 4.0 (in comparision to cylinders of height-to-diameter ratio of 2.0) was observed. The curves presented in the paper indicate that the fall in strength ratio versus height-to-diameter ratio is quite steep, even at height-to-diameter ratios greater than 4.0.

In 1941, Troxell (5) investigated the effect of some other capping materials such as Hydrostone (a gypsum product), Castite (a sulfur-silica mixture), oiled steel shot, dry steel shot, and Plaster of Paris. He concluded that, regardless of the end conditions of the cylinders before capping, a higher strength and greater degree of uniformity of strength for the same quality of concrete are obtained with Hydrostone or Castite caps. Plaster of Paris caps gave lower strengths, especially for high-strength concrete.

A study by Johnson (6) in 1942 on the effect of height of test specimens on compressive strength reinforced previous observations. Johnson concluded that a correction factor should be applied for specimens for which the length is greater than twice the diameter.

Price (9) mentions specimen geometry as one of the factors influencing compressive strength of concrete test specimens.

In 1956, Neville (10) reported results on the testing of cube specimens of 2.78 in., 5 in., and 6 in. The mean strength of 2.78-in. cubes was higher than that of either the 5-in. or the 6-in. cubes.

Werner (11), in 1958, studied the effect of capping materials on the compressive strength of concrete cylinders and concluded that capping materials did have a distinct effect on the strength.

In 1964, Newman and Lachance (12) reported an extensive study conducted at the Imperial College in London. They investigated mainly the deformational behaviour of specimens with different geometries (prisms 4 in. square with heights ranging from 4 in. to 20 in.). They measured lateral and longitudinal deformations. The lateral deformation at about mid-height was most for the smallest specimens, gradually diminishing with increasing specimen height. They showed that tangential stresses were induced at the ends of the specimen, but dropped rapidly with increasing distance from the ends. Axial stresses again were seldom uniform, and they concluded that axial stress concentrations could occur.

In 1965, Hughes and Bahramian (13) recognized the need for a modified uniaxial test. They used 4-in. cubes and prisms 4 in. by 4 in. by 9-5/8 in., and initially introduced interlayers of polytetrafluoroethylene between the specimens and the bearing platen, but finally decided on using pads consisting of a polyester film (Melinex, gauge 100), a grease containing 3 percent molybdenum disulphide (Molyslip), and a hardened aluminum sheet, 0.003 in. thick (MGA). They observed that lateral strains were reduced considerably at some stress levels as a result of the MGA pads.

In 1969, Kupfer, Hilsdorf and Rusch (14) developed a steel brush device with filaments 5 mm. by 3mm. and spaced 0.2 mm. apart. The idea was that the bristles would produce axial loads, but, because of their own small lateral stiffness, would deflect, and therefore would not produce lateral restraint at the specimen ends. A comparable device had been developed earlier by the Kaiser-Wilhelm Institute (15). It consisted of a cone with base angles equal to the angle of

friction between steel and concrete; the end effect would be to produce uniaxial compression. However, this method, though suitable for testing metals, was not suited to concrete because of the difficulty in evaluating the friction between steel and concrete consistently.

In 1973, Schickert (16) published a detailed study on the influence of frictional restraint on fracture modes. He used steel brushes and aluminum sheets to minimize end friction and showed that with aluminum sheets, the strength of test specimens was 92 percent of the compressive strength obtained using steel platens. He also showed that steel brushes reduced the strength to 81 percent of that obtained using steel platens.

Most recently, Basunbul (17) concluded from his work that for test specimens of height-to-diameter greater than or equal to 2, the frictional constraint had no apparent influence on strength, which is contrary to what other investigators have found.

In summary, the apparent ultimate strength of concrete and the lateral and longitudinal stress distributions within it are significantly affected by end frictional conditions, and by the geometry of the specimen.

CHAPTER 2

SCOPE OF INVESTIGATION

The present investigation was designed to evaluate a method for determining the strength of concrete in truly unconfined uniaxial compression and then to test the method in the context of a design application.

Data of earlier investigators suggest that the apparent strength of concrete in compression (fc) is inversely proportional to the aspect ratio (H/D) of the test specimen; that is, fc vs. H/D is a rectangular hyperbola translated from the origin in the direction of fc. If so, a simple variable transformation of the form, $x = 1/x$, should yield a straight line with a y-intercept equal to the displacement of the horizontal asymptote of the corresponding rectangular hyperbola along the y-axis. The fact that correction factors to be applied to strengths obtained from cores of H/D less than 2 (ASTM C42: Standard Method of Test for Obtaining and Testing Drilled Cores and Sawed Beams of Concrete (1)) are approximately linear following variable transformation supports this hypothesis.

In order to test this hypothesis, five sets of six replications of cylinders of six different aspect ratios, all cast from a single normal-weight concrete mixture, and a similar set cast from a single light-weight concrete mixture, were to be tested in compression in accordance with applicable portions of ASTM C39 (1). Among the five sets of normal-weight concrete cylinders, end conditions were to be altered to vary the frictional restraint. Coincidentally, the elastic modulus and Poisson's ratio were to be measured for a

representative set.

Finally, ultimate stresses determined in a field of unconfined uniaxial compression in a structural element were to be compared with the unconfined cylinder strengths estimated as described above. The classic specimen of Hognestad, Hanson, and McHenry (23) was to be used for this purpose.

CHAPTER 3

MATERIALS, MIXTURES, SPECIMENS, AND INSTRUMENTATION

3.1 Materials

3.1.1 Fine Aggregates

The fine aggregate used was a uniformly graded local sand from the Kaw River Valley. The sand was first dried in air, and then dried in an oven for 24 hours, sieved through a standard No. 4 sieve, and stored in sealed containers.

3.1.2 Coarse Aggregates

The coarse aggregate used was a locally available pseudo-quartzite for normal-weight concrete, and a locally manufactured expanded shale for light-weight concrete. Both aggregates were uniformly graded to a maximum size of 3/4 in..

3.1.3 Cement

The cement used was ordinary portland cement, Type I. It was stored in sealed drums pending use.

3.2 Molds

Molds for cylinders with different diameter-to-height ratios were made from PVC Schedule 80/40 pipes of internal diameter 2-7/8 inches.

We proposed to make six different sizes of cylinders with diameter-to-height ratios ranging from approximately 0.17 to 1.00. Six cylinders molds of each size were fabricated into a gang of 36 molds for any one set. A shop drawing of the gang mold is shown in Figure 1. Figure 2A is a photograph of the assembled mold. Figure 2B shows the hold-down detail.

The beam mold consisted of a wooden base and 3/4-in.-thick

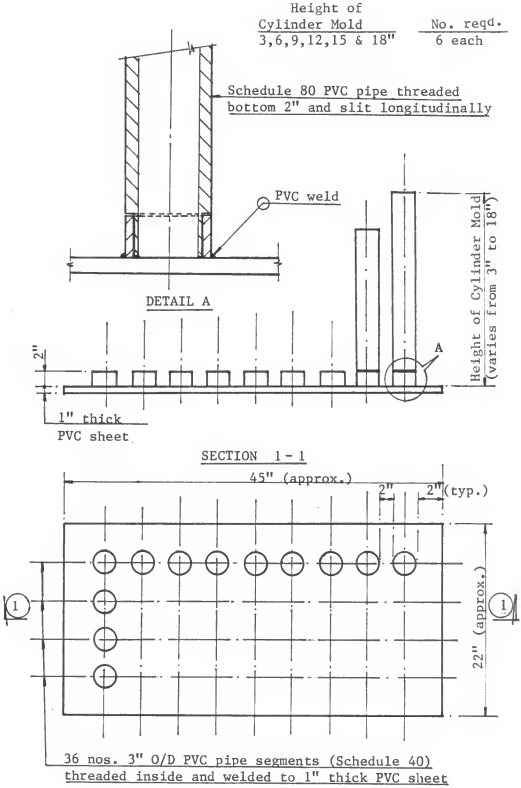

General Arrangement of Cylinder Molds

Figure 1

Figure 2A: Assembled Cylinder Molds.

Figure 2B: Hold-Down Detail of Mold.

plexiglass walls. The plexiglass was fixed to the base with 1/2-in. angles and round-head screws 1-1/2 in. long. The joints were sealed with tape to prevent leakage.

Molds for companion cylinders to the beams were paraffin-coated paper molds complying with ASTM C39 (1).

The inner surfaces of the PVC cylinder molds and the beam forms were oiled lightly before concreting.

3.3 Proportioning, Mixing, and Curing

3.3.1 Mix Design

The mixture proportions used for normal-weight, high-strength concrete were those developed and used in earlier work on the investigation of the stress-block of high-strength concrete at Kansas State University (24). Those used for light-weight concrete were recommended by the aggregate manufacturer. Proportions and pertinent properties are shown in the following tabulation:

Material	Weight of material per cft. of concrete, lb.	
	Normal-weight	Light-weight
Portland cement (c)	27.5	35.2
Water (w)	9.0	12.3
Coarse aggregate	49.7	31.9
Fine aggregate	60.9	49.0
Property		
w/c, by wt.	0.33	0.35
Slump, in.	2±1/2	2±1/2
fc, psi	9600	7000

3.3.2 Mixing and Casting Procedures

The batched ingredients were mixed in a power-driven, rotary-drum mixer of 3.5 cubic feet capacity.

To minimize variation among batches, uniform procedures were followed, especially when specimens were cast from two separate batches of concrete, as in the case of the beam specimens.

A "buttermix" with a quarter cubic foot of concrete was mixed and discarded before the first full batch was mixed, to eliminate differences between the first batch and subsequent batches.

Dry ingredients were mixed for 30 seconds. Water was poured in gradually over the next 30 seconds, and mixing was continued for 4 minutes. The concrete was then discharged into a large pre-dampened pan, and a standard slump test was performed immediately thereafter.

The concrete in cylinder molds was tamped with a 3/8-in. rod with rounded head as the concrete was placed in layers of about 3 inches. Subsequently the molds were vibrated on a shaking table. The molds had been secured to the vibrating table prior to concreting. The formwork of the beam and its companion cylinder molds was filled to half the depth with concrete from the first batch and finished with material from the second.

Five sets of cylinders were fabricated with normal-weight concrete and one with light-weight concrete.

3.3.3 Curing

All specimens were covered with polyethylene sheets to prevent loss of moisture.

The cylinder specimens were stripped from their molds after 24

hours and put in a standard curing room. The cylinders in any particular batch were subsequently removed from the curing room on the same day and kept in the laboratory until time of test.

The beam specimens could not be stripped the next day and handled, due to strength considerations. The beams were stripped after a period of seven days after casting. The companion cylinders were stripped simultaneously and placed in the curing room. The beam specimens and its companion cylinders were cured in exactly the same manner for the same period of time.

3.4 Specimen Preparation

The ends of the test specimens were prepared as follows:

Cylinder Set	Description
1	Normal-weight concrete. Standard sulfur-capped with residual oil.
2	Normal-weight concrete. Standard sulfur-capped with powdered tetrafluoroethylene.
3	Normal-weight concrete. Standard sulfur-capped without residual oil. Ends degreased.
4	Normal-weight concrete. Ground surface without powdered tetrafluoroethylene. Ends degreased.
5	Normal-weight concrete. Ground surface with tetrafluoroethylene.
6	Light-weight concrete. Standard sulfur-capped with residual oil.

A given set of 36 cylinders (six different heights, six of each size) were taken out of the curing room at the same time, and left to

dry out for a day under ambient room conditions.

Sulfur-capping was done in accordance with ASTM C39 (1). The capping base was provided with new guides for cylinders of average diameter 2-7/8 in.

The capping was checked for perpendicularity to the long axis of the specimen by placing the capped specimen on a plane horizontal surface and checking it with a spirit level. If the bubble shifted from the center, the specimen was re-capped. The smallest specimens posed difficulty in capping and had to be capped several times before satisfactory results were obtained.

Two sets of cylinders had ground surfaces. The surface cast against the PVC plate was already plane and perpendicular to the long axis of the specimen. This end of the specimen was chucked up in a lathe. The other end was faced with a diamond cutting tool at a high r.p.m. and slow cross-feed. The cuts were made in small increments, and the resultant end surfaces were extremely smooth to the touch. No coolant was required for the facing operation.

In this operation, the smaller cylinders posed no problem. But with the larger sized cylinders, there remained a distinct possibility that the cylinder could slip out of the chuck and be damaged in the process. A steady-rest was therefore fabricated to accomodate lateral forces induced in the cutting process.

3.5 Instrumentation

Lateral and axial strains were measured to evaluate the modulus of elasticity, E, and Poisson's ratio for cylinders of different diameter-to-height ratios.

Six cylinders of different heights from Cylinder Set 3 (sulfur-capped, without residual oil) were instrumented for this purpose. Two axial gages 180 degrees apart and two lateral gages diametrically opposite to each other at mid-height were used.

Electric-resistance strain gages, 2 in. long, were installed in accordance with the recommendations of the manufacturer.

The beam specimens were instrumented following the same procedures. The gages were located as shown in Figure B1. One 3-in.-by-6-in. companion cylinder was also instrumented with two axial strain gages 180 degrees apart.

CHAPTER 4

TEST PROCEDURES

4.1 Cylinder Specimens

Cylinder specimens with prepared end surfaces were marked individually for identification. Three diameter measurements were taken with a caliper reading to the nearest 0.001 in., and an average of the three was computed. This average diameter was used in all subsequent computation. Measurements of height were also recorded. For capped surfaces, the height was taken to include the caps. The cylinder was centered in the testing machine to the best of our ability. For centering the specimen, we relied on markings on the base plate. Two lines intersecting at 90 degrees, and tangent to a circle of diameter 2-7/8 in., were drawn on the base plate with a carbide-tipped scriber. A small steel angle section was aligned with the etching on the base plate. The cylinder was brought into position so that its sides touched the angle. The angle was removed before loading.

The difficulty with this procedure was that the cylinders were not perfectly circular in cross-section, as is evident from the data presented in Tables A1 to A6 (Appendix A). The specimens may not have been truly centered, but the ultimate stress values which do not have a wide standard deviation indicate that the technique was sound.

The testing machine used was a load-controlled Emery-Tatnall 300,000-lb. hydraulic testing machine. The machine platen was brought to bear on the cylinder, and load was applied at a uniform rate to failure. The load at failure was recorded and divided by the cross-

sectional area to give the "uniaxial" compressive stress.

Strain data for the cylindrical specimens of different diameter-to-height ratio were recorded with a Vishay-Ellis Digital Strain Indicator. The cylinders were loaded to predetermined load levels with approximately equal increments, and the strains corresponding to particular loads were recorded automatically.

Since failure was sudden in most cases, it was not possible to record the strains corresponding to the ultimate load. However, in most cases, we were successful in recording strain data close to failure.

4.2 Beam Specimens

Loading on the beam consisted of a major thrust, P1, and a minor thrust, P2, as shown in Figure B1. The objective was to load the beam in a manner such that the neutral axis coincided with the outer face of the specimen. The approximate zero strain surface represents the neutral axis of the flexural member while the opposite face represents the extreme compressive side.

The beam was placed in a standing position in the Emery-Tatnall machine to apply the major load P1. The minor load P2 was applied using a hydraulic ram and a yoke as shown in Figure B4. The hydraulic ram was placed in series with a load cell. The load cell was hooked to a digital readout which displayed readings to the nearest 10 lb.

The loading yoke was secured to the machine, and the load cell was bolted to the yoke, to prevent damage to either at failure.

An initial major thrust was applied, and the yoke was placed in position. This was done to prevent tension developing on the outer

face due to the weight of the yoke.

The strain indicator was zeroed at this point, and initial readings at this load level were recorded. The major thrust was then increased. The hydraulic ram was operated to apply an eccentric load until the indicated strains at the outer face were zero. At this point, the minor load and the corresponding compressive strains were recorded. This procedure was repeated incrementally until failure occurred.

The recorded load-strain data and computations to arrive at a value for compressive stress of concrete at failure, along with test results of the 3-in.-by-6-in. companion cylinders are presented in Tables A15 through A22.

4.2.1 Difficulties and Precautions

The beam specimens weighed over 300 lb. Hence, handling was a problem. Moreover, the mid-section, the test region, was unreinforced (as shown in Figure B2), and extra caution had to be exercised in order not to fracture this region in transporting the beam.

Centering the beam in the machine, so that the load P1 could be applied concentrically, was another major problem. The beam had a tendency to tilt slightly as a result of defective form-work. This difficulty was overcome by capping the loading region of the beam with Hydrostone, and levelling it with a spirit level.

Keeping the strain at zero on the outer face was also a difficult task. This was achieved, however, to some degree of accuracy by careful operation of the hydraulic ram.

The digital display for the minor load usually jumped around with a variation of 40 lb. between the highest and lowest readings. Aver-

ages of the highest and lowest readings were interpreted as the operative value of P2.

Following failure, the entire system was unstable; so everything was slung with rope from the testing machine cross-head.

CHAPTER 5

TEST RESULTS

5.1 Cylindrical Specimens with Varying Diameter-to-Height Ratios and End Conditions

5.1.1 Normal-Weight Concrete

The results obtained from the five sets of cylinders of normal-weight concrete are presented in Tables A1 through A5 (Appendix A).

In all cases, fc is the mean of stresses corresponding to ultimate loads in cylinders identified as "B" (standard cylinders).

Individual cylinder strengths, f, are divided by fc. This ratio, f/fc is plotted against D/H. The plots are shown in Figures 3 through 7.

A linear regression analysis yields the following straight-line fits with corresponding correlation coefficients, R:

Cylinder Set	Description	Eqn. of st. line y = f/fc & x = D/H	R
1	Sulfur-capped, with residual oil	y = 0.347x + 0.834	0.957
2	Sulfur-capped, with TFE	y = 0.169x + 0.884	0.742
3	Sulfur-capped, without residual oil	y = 0.301x + 0.863	0.941
4	Ground surface, without TFE	y = 0.346x + 0.847	0.975
5	Ground surface, with TFE	y = 0.192x + 0.893	0.855

In general, a linear fit seems to be good, judging from the high correlation coefficients. However, it may be noticed that Set 5 and especially Set 2 have a lower correlation coefficient than the other three sets. A segmental linear fit was tried for Set 2. Figure 4A

shows one segment of the fit (D/H = 0.85 excluded). The equation of the line of best fit is y = 0.373x + 0.833, with a higher correlation coefficient of 0.804. Interestingly enough, the intercept is much lower (0.833 against 0.884), which makes it comparable to sets without TFE. It appears that the effect of TFE is most pronounced for the smallest cylinders. In the complete absence of friction we would expect a straight line fit parallel to the x-axis, of the form y = c, c being the intercept of the y-axis.

The intercept in all five cases lies between 0.834 and 0.893. The intercept represents the correction factor needed to convert the ultimate strength of the standard cylinder to the true uniaxial compressive strength.

The strengths of cylinders cast in paper molds indicate a reduction in strength as compared to cylinders cast in PVC molds. In Table A1, where the end conditions were exactly the same for cylinders cast in PVC and paper molds, a reduction in strength of 2.2 percent is indicated. This result is consistent with the findings of Burmeister (25).

5.1.2 Light-Weight Concrete

Results for the set cast with light-weight concrete are presented in Table A6, and a plot of these results is shown in Figure 8.

The analytical procedure followed is the same as for Cylinder Sets 1 through 5 for normal-weight concrete.

A linear regression analysis of the plot of f/fc (y) versus D/H (x) yields:

y = 0.161x + 0.886, with a correlation coefficient of 0.77.

The intercept is higher than that obtained for normal-weight concrete (0.886 compared to 0.834) with cylinders having identical end conditions. On inspection of the plot, it is seen that a segmental linear fit would be more appropriate, giving a higher correlation coefficient and a lower intercept.

We did notice a peculiar phenomenon in light-weight concrete. The ultimate stresses in cylinders identified as "A" and "B" were approximately the same.

Two sets of nine cylinders, of diameter-to-height ratios of 0.5 and 1.0 cast with light-weight aggregate were cast. They were capped with sulfur and tested. The strengths were identical again. The results are shown in Table A7.

The behavior of light-weight concrete seems to be entirely different to normal-weight concrete, in so far as cylinders of D/H ratios of 0.5 and 1.0 are concerned. The established difference of 15 percent in D/H ratios of 0.5 and 1.0 for normal-weight concrete is not noticed in light-weight concrete.

5.2 Mechanical Properties of Cylinders with Varying Diameter-to-Height Ratios

The stress-strain data are presented in Tables A8 to A14. These cylinders were taken from Set 3.

The plots of axial stress vs. axial strain and axial stress vs. lateral strain are presented in Figures 9 through 21.

Modulus of elasticity, E, and Poisson's ratio are found at 0.45fc. The results are tabulated on the next page.

D/H	Modulus of Elasticity, E, psi	Poisson's Ratio
0.16	4.8 E +06	0.21
0.19	4.9 E +06	0.22
0.23	5.1 E +06	0.23
0.31	5.2 E +06	0.25
0.45	5.3 E +06	*
0.85	5.4 E +06	0.22

* Lateral strain gage malfunction.

The standard sulfur-capped 3-in.-by-6-in. cylinder cast in a paper mold gave a modulus of elasticity value of 5.1 E +06 psi (ACI formula gives 4.9 E +06 psi), and a Poisson's ratio of 0.22.

The results indicate a significant difference in the modulus of elasticity with change in specimen geometry, about 11 percent between cylinders of D/H = 0.85 and 0.16.

Poisson's ratio at mid-height increases from 0.21 at D/H = 0.16 to 0.25 at D/H = 0.31. Lateral strains in the cylinder with D/H = 0.45 could not be determined due to strain gage malfunction. However, the cylinder with D/H = 0.85 yielded a Poisson's ratio of 0.22, which does not tally with the trend indicated by the other cylinders. Newman and Lachance (12) have reported similar results. In general, the differences in Poisson's ratio and in lateral strain at mid-height for varying height of specimens is about 16 percent for the concrete used in the test.

5.3 Beam and Companion Cylinder Specimens

5.3.1 Normal-weight concrete

The method of analysis is presented in Appendix B.

The values of df/dϵ and dm/dϵ are computed using the first derivative of the equation of the curve of best fit for the plots of f vs. ϵ and m vs. ϵ. A quadratic regression analysis was done (Tables A16 and A17), and the residuals indicate that the predictive equations are satisfactory.

The compressive stresses at the inner face of the beam, computed from an average of the two stress values obtained from the equations

$$fc = \epsilon \left(df/d\epsilon \right) + f,$$

and $$fc = \epsilon \left(dm/d\epsilon \right) + 2m,$$

are presented in Table A15. Hence, compressive strain, ϵ, can be plotted against fc (average) (Figure 22).

A standard sulfur-capped 3-in.-by-6-in. companion cylinder cast in a paper mold was also instrumented and tested. The stress-strain data are presented in Table A18. These stress-strain values are also plotted in Figure 22. Ultimate stress values of all the companion cylinders (including the one which was instrumented) are presented below:

Cylinder Set	Ultimate load, P, lb.	Area, A, sq. in.	Stress, P/A, psi	Mean, psi	Std. Dev., psi
1	54400		7690		
2	59000		8350		
3	53400	7.07	7550	7870	350
4	55800		7890		

The final compressive stress in the beam that could be computed from the available data was at a major load , P1, of 115000 lb. A

reasonable procedure to find the ultimate compressive stress would be to extrapolate the preceding data. The differences indicate that the ultimate compressive stress in the beam would be (7260 + 70) equal to 7330 psi. This is a 7 percent reduction from the ultimate compressive stress of the 3-in.-by-6-in. cylinders.

This percent value does not reflect the predicted "true" uniaxial compressive stress value, which was found to be about 15 percent lower than the ultimate compressive strength of cylinders with D/H approximating 0.5.

There are two factors for this, namely, (a) the difference in strengths of cylinders cast in cardboard and paper molds PVC molds; and, (b) the test region in the beam was 5 in. by 5 in. by 16 in., giving D/H value of 0.31.

From Table A1, it may be observed that reduction for factor (a) above is about 2.2 percent, and the additional reduction for factor (b), from Figure 3, is 10 percent. This adds up to an additional 12.2 percent, over and above the 7 percent already shown, making a total reduction of about 19 percent of the compressive strength of the standard cylinder.

Hence, it may be reasonably argued that the reduction in compressive strength is a valid proposition, and a reduction of about 15 percent is not at all unreasonable.

5.3.2 Light-weight concrete

Computations similar to those made for the beam specimen made with normal-weight concrete are presented in Tables A19 through A21. Stress-strain data for a companion cylinder is tabulated in Table A22.

Results for all the companion cylinders are presented below.

Cylinder #	Ultimate load, P, lb.	Area, A, sq. in.	Stress, P/A, psi	Mean, psi	Std. Dev., psi
1	40200		5690		
2	41900		5930		
3	40900	7.07	5790	5950	220
4	43200		6110		
5	44000		6220		

However, the value computed for ultimate compressive strength in the beam is 7220 psi, greater than the compressive strength of 5950 psi computed in the standard 3-in.-by-6-in. cylinders.

Numerical computation seems to be correct. The raw data also look good, and so do the polynomial curve-fits. The reason for this apparent anomaly is not clear.

CHAPTER 6

CONCLUSIONS AND RECOMMENDATIONS

The test results of Cylinder Sets 1 through 5 cast in normal-weight concrete indicate that the strength of concrete determined by the standard cylinder test is higher than its strength in truly uniaxial compression by some 11 to 17 percent, based on linear regression analysis. When the data from Cylinder Set 2 are subjected to a segmental linear regression analysis, the correlation coefficient improves, and the standard cylinder strength becomes 17 percent higher than the estimated strength in unconfined compression. The data from Cylinder Set 5 also appear to be segmental.

The apparent discontinuity in the slopes of these two data sets is not understood. The bearing surfaces of the cylinders of both sets were lubricated with powdered tetrafluoroethylene, but it is not clear that that fact is all or part of the cause of the anomaly. Further research is necessary if it is to be understood.

Test results for Cylinder Set 6 cast in light-weight concrete indicate a reduction of 11 percent, based on linear regression analysis. Based on a segmental linear analysis, the reduction is 17 percent, with a corresponding improvement in the correlation coefficient. Replicate testing indicates that the anomaly is real, but the cause is not yet clear.

Apparently, the strength of concrete in truly unconfined compression is of the order of 85 percent of the strength determined from standard cylinders tested in accordance with ASTM C39 (1).

In the case of normal-weight concrete, ultimate stress determined

in the Hognestad-Hanson-McHenry structural element compared well with the estimated strength in unconfined compression. In the case of light-weight concrete, the ultimate stress was significantly higher than the estimated strength in unconfined compression. Again, the apparent anomaly in the latter case is not understood, and further work is needed to clarify it.

The measured secant modulus of elasticity is affected significantly by specimen geometry. In this instance, an increase in aspect ratio of three resulted in a reduction of about 10 percent in the secant modulus. Over the same range of aspect ratio, Poisson's ratio varied between 0.21 and 0.25.

The evidence presented here strongly suggests that standard test methods for determining the strength of concrete in compression and the secant modulus of elasticity are significantly unconservative for normal-weight concrete, though not necessarily so for light-weight concrete. It is recommended that research be continued to explain the anomalies encountered, to identify and explain other anomalies, and ultimately to generate an extensive data base as a significant resource for review and revision of methods of test and design codes.

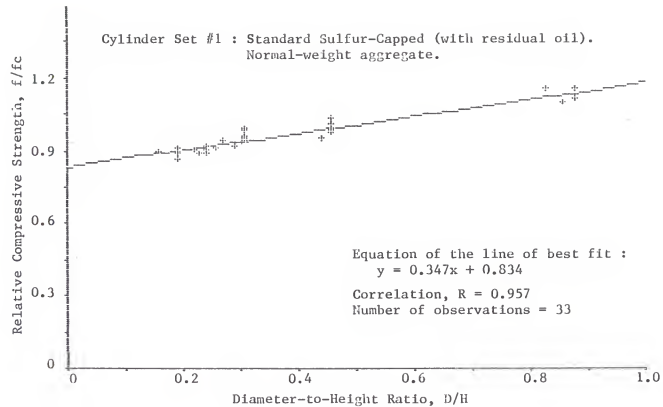

Figure 3: Influence of Diameter-to-Height on Relative Compressive Strength.

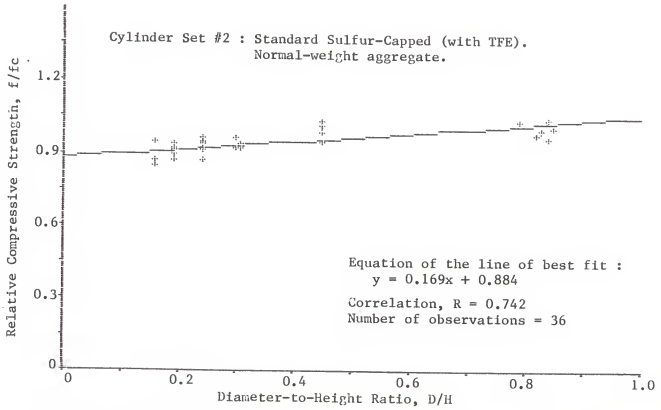

Figure 4: Influence of Diameter-to-Height on Relative Compressive Strength.

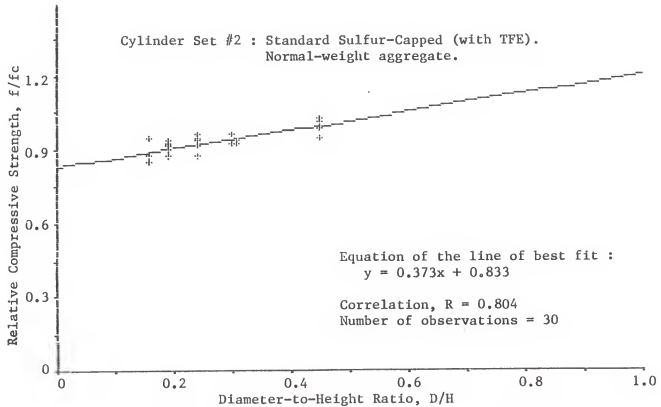

Figure 4A: Linear Regression for Data in Left-Half of Figure 4.

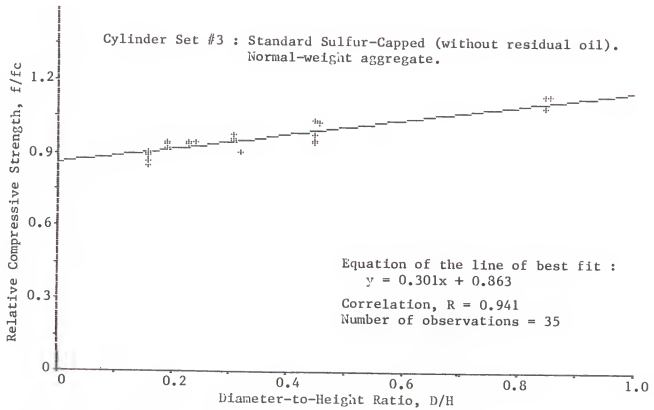

Figure 5: Influence of Diameter-to-Height on Relative Compressive Strength

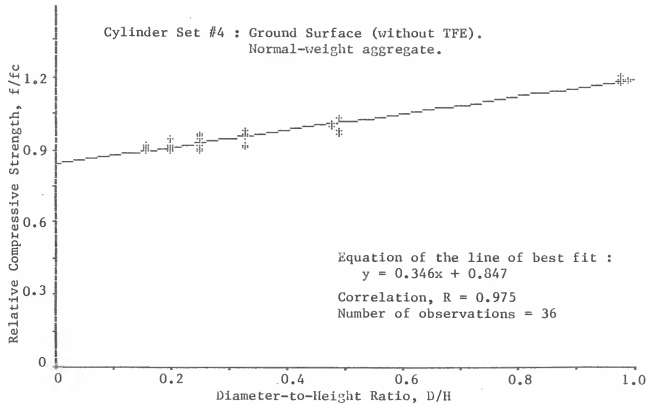

Figure 6: Influence of Diameter-to-Height on Relative Compressive Strength

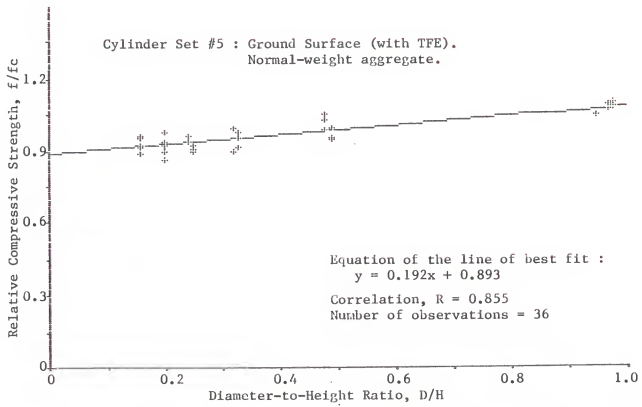

Figure 7: Influence of Diameter-to-Height on Relative Compressive Strength

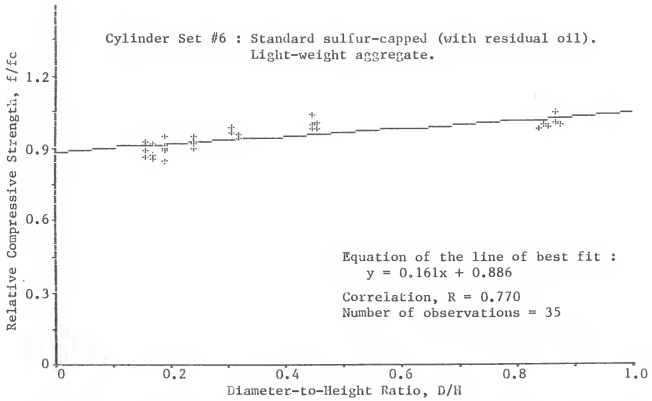

Figure 8: Influence of Diameter-to-Height on Relative Compressive Strength

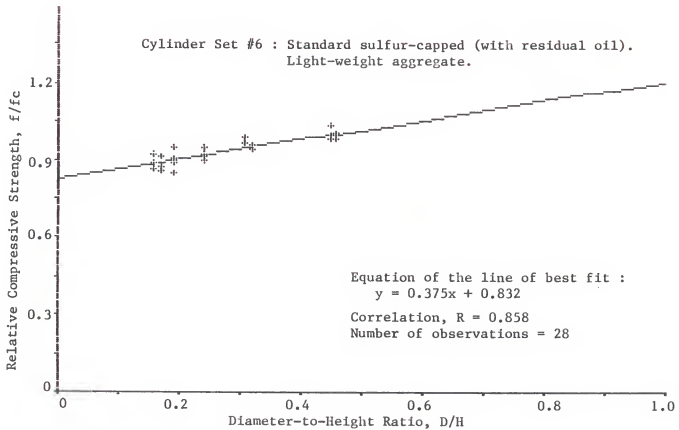

Figure 8A: Linear Regression for Data in Left-Half of Figure 8.

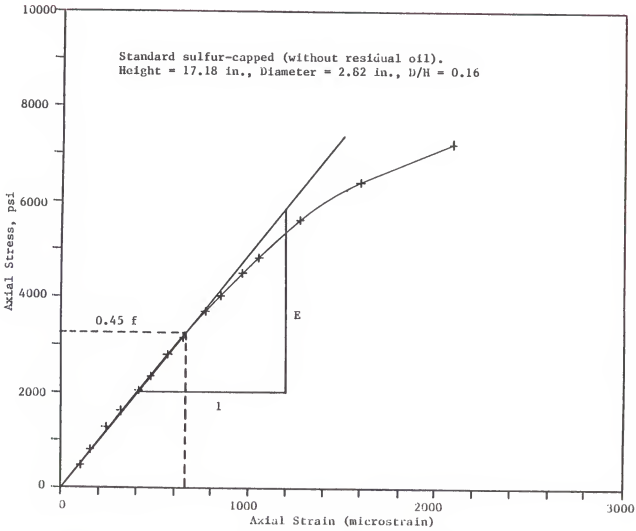

Figure 9: Stress vs. Axial Strain Curve for Cylinder with D/H = 0.16.

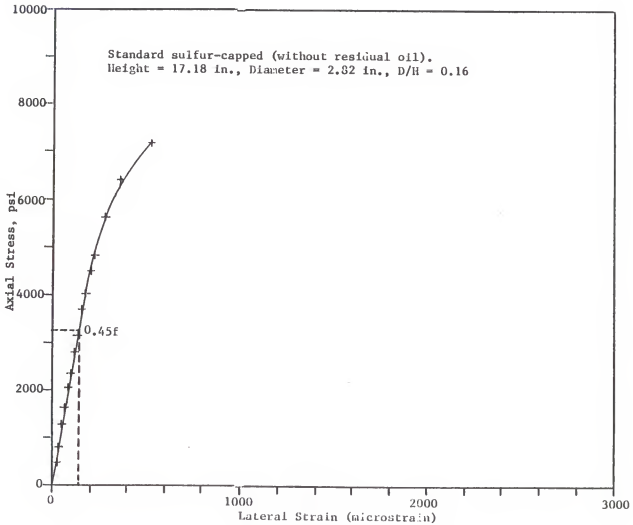

Figure 10: Stress vs. Lateral Strain Curve for Cylinder with D/H = 0.16.

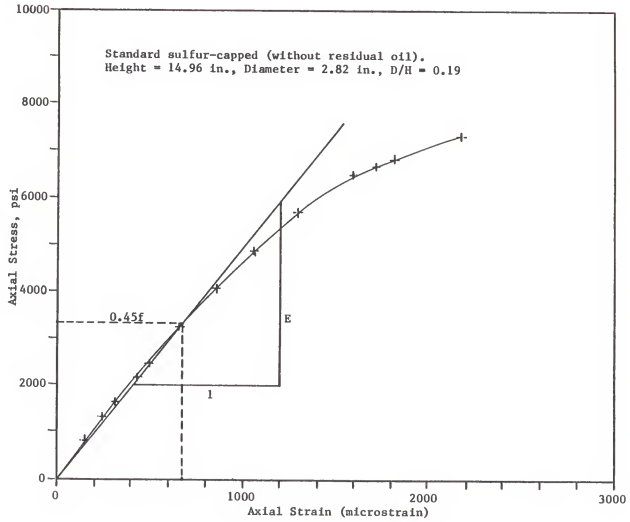

Figure 11: Stress vs. Axial Strain Curve for Cylinder with D/H = 0.19.

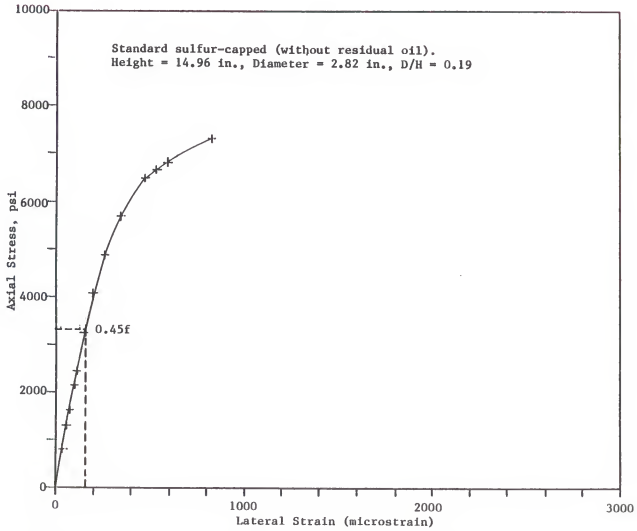

Figure 12: Stress vs. Lateral Strain Curve for Cylinder with D/H = 0.19.

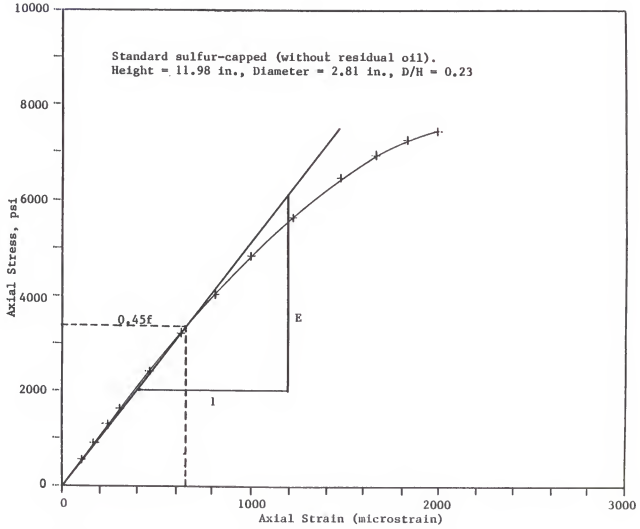

Figure 13: Stress vs. Axial Strain Curve for Cylinder with D/H = 0.23.

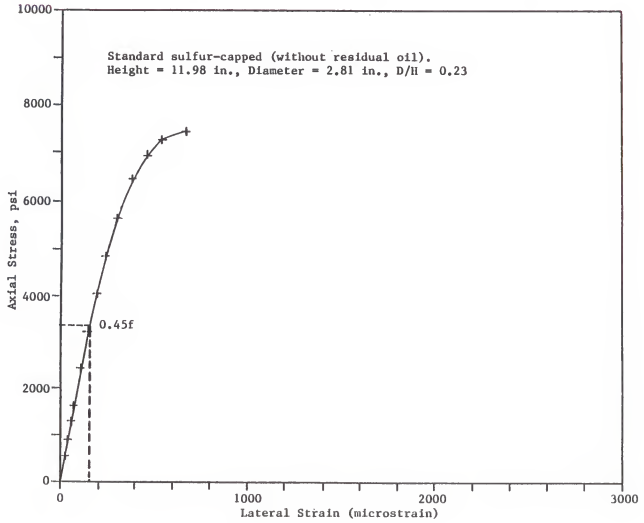

Figure 14: Stress vs. Lateral Strain Curve for Cylinder with D/H = 0.23.

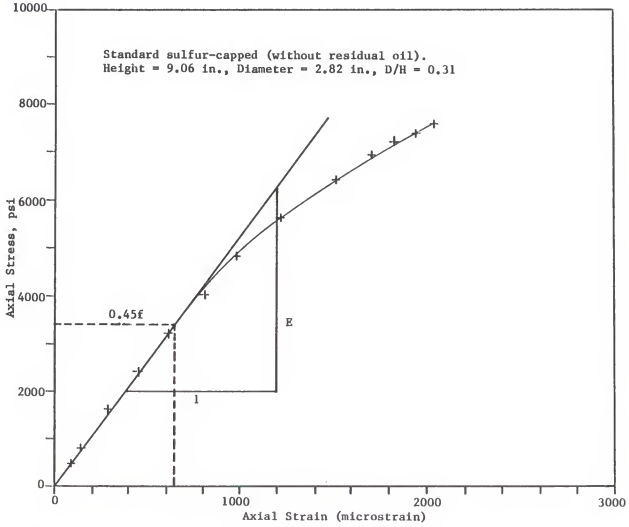

Figure 15: Stress vs. Axial Strain Curve for Cylinder with D/H = 0.31.

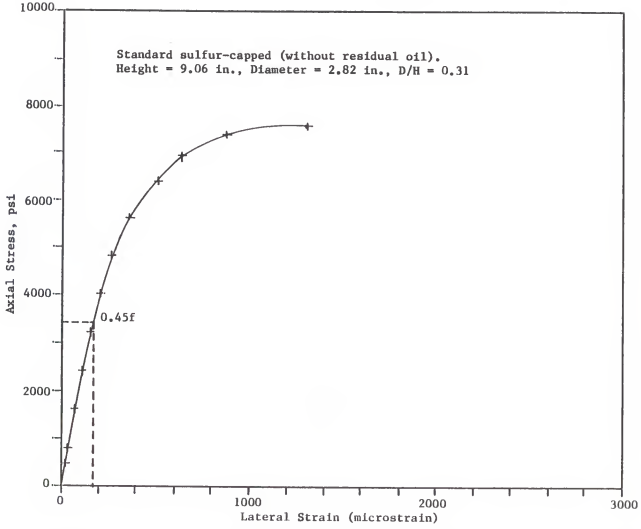

Figure 16: Stress vs. Lateral Strain Curve for Cylinder with D/H = 0.31.

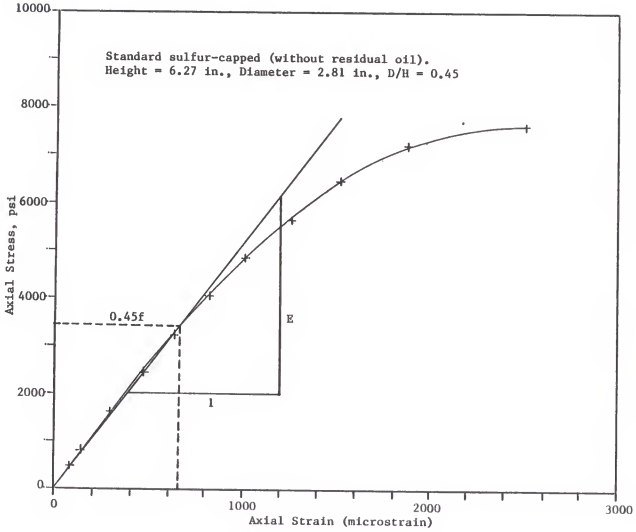

Figure 17: Stress vs. Axial Strain Curve for Cylinder with D/H = 0.45.

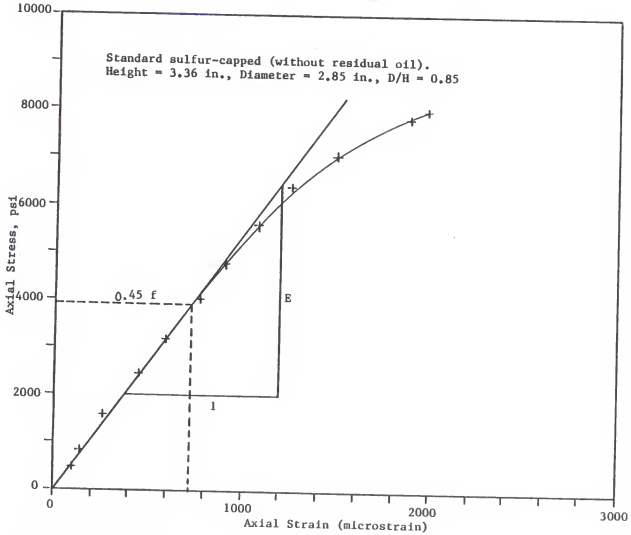

Figure 18: Stress vs. Axial Strain Curve for Cylinder with D/H = 0.85.

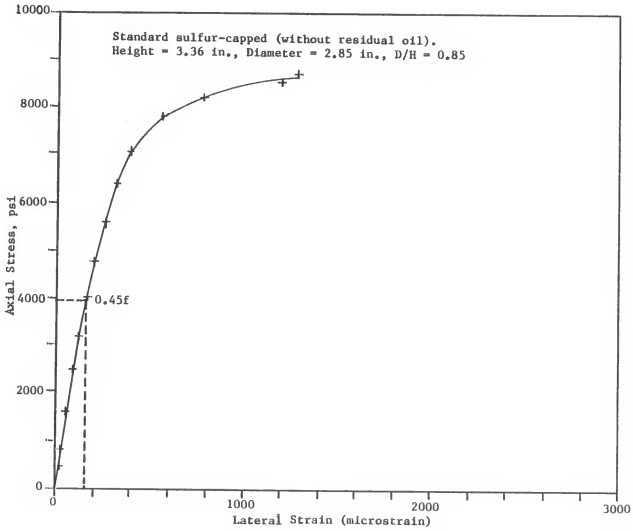

Figure 19: Stress vs. Lateral Strain Curve for Cylinder with D/H = 0.85.

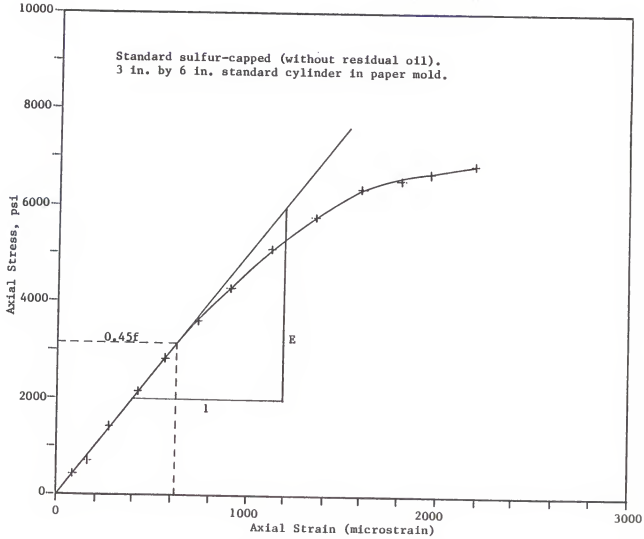

Figure 20: Stress vs. Axial Strain Curve for 3 in. by 6 in. Standard Cylinder.

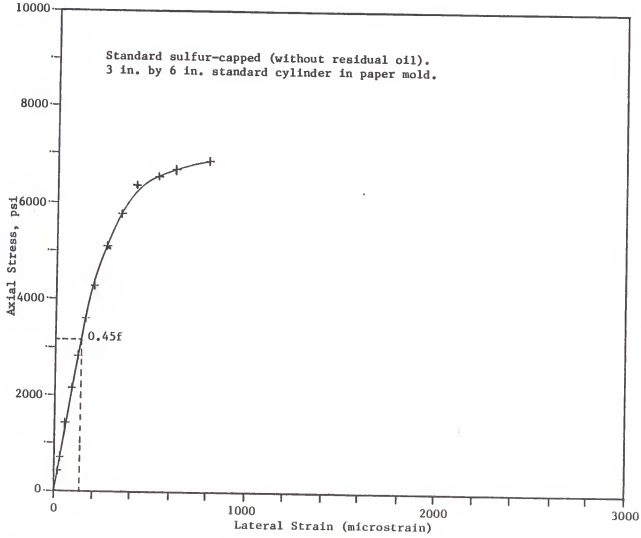

Figure 21: Stress vs. Lateral Strain Curve for 3 in. by 6 in. Standard Cylinder.

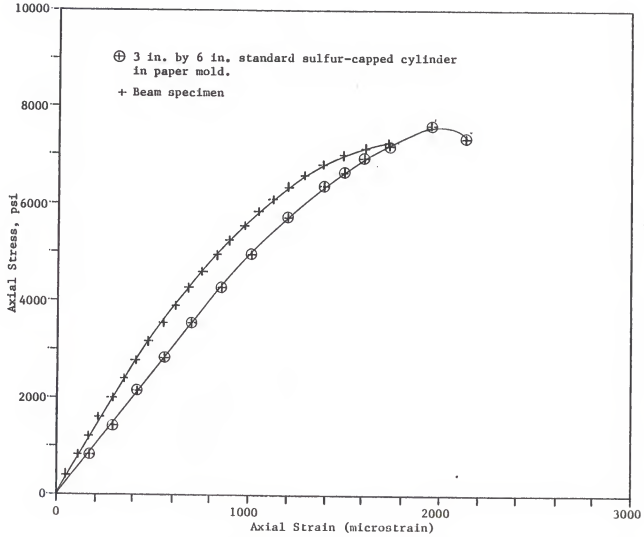

Figure 22: Comparision of Stress vs. Axial Strain Curves for Beam Specimen and 3 in. by 6 in. Companion Cylinder (Normal-weight Concrete).

APPENDIX A

TABLES

Table 81 : Cylinder Set #1 : Sulfur-Capped (with residual oil), PVC Molds.
Normal-weight aggregate.

Specimen I.D.	Specimen Dimensions, in.					D/H	Area, sq. in.	Ult. Load, P,lb.	f=P/A	f'fc	Mean psi	Std. Dev. psi
	Dia.,D1	Dia.,D2	Dia.,D3	Avg Dia.,D	Height,H							
1A	2.850	2.800	2.825	2.825	3.300	0.88	6.27	56000	8930	1.12		
	2.850	2.750	2.800	2.800	3.230	0.87	6.16	62600*	8510*	1.07*		
	2.825	2.850	2.850	2.842	3.230	0.88	6.34	56500	8910	1.12	9050	190
	2.800	2.875	2.800	2.825	3.280	0.86	6.27	55800	8900	1.11		
	2.800	2.800	2.850	2.817	3.280	0.83	6.23	67500	9240	1.16		
	2.800	2.850	2.850	2.833	3.210	0.88	6.30	58500	9280	1.16		
1B	2.825	2.800	2.825	2.817	6.120	0.46	6.23	50600	8020	1.00		
	2.825	2.850	2.825	2.833	6.440	0.44	6.30	48100	7630	0.96		
	2.750	2.825	2.850	2.808	6.160	0.46	6.19	51600	8330	1.04	fc	
	2.850	2.825	2.750	2.808	6.160	0.46	6.19	48700	7860	0.98	7970	240
	2.800	2.750	2.825	2.792	6.110	0.46	6.12	49700	8120	1.02		
	2.850	2.850	2.800	2.833	6.100	0.46	6.30	49600	7870	0.99		
1C	2.850	2.776	2.825	2.817	8.980	0.31	6.23	49600	7960	1.00		
	2.800	2.800	2.825	2.808	9.000	0.31	6.19	47300	7640	0.96		
	2.800	2.850	2.825	2.825	9.000	0.31	6.27	49700	7930	0.99	7760	150
	2.850	2.825	2.800	2.825	9.000	0.31	6.27	48200	7690	0.96		
	2.800	2.876	2.850	2.842	9.100	0.31	6.34	49000	7730	0.97		
	2.776	2.800	2.850	2.808	9.080	0.31	6.19	47100	7600	0.95		
1D	2.776	2.800	2.850	2.808	11.850	0.24	6.19	46100	7440	0.93		
	2.826	2.800	2.850	2.826	11.860	0.24	6.27	45500	7260	0.91		
	2.776	2.850	2.826	2.817	11.910	0.24	6.23	45300	7270	0.91	7250	120
	2.826	2.800	2.825	2.817	11.900	0.24	6.23	44500	7140	0.89		
	2.825	2.800	2.825	2.817	11.830	0.24	6.23	45500	7300	0.91		
	2.876	2.850	2.776	2.833	11.810	0.24	6.30	44800	7110	0.89		
1E	2.875	2.825	2.776	2.826	14.760	0.19	6.27	43700	6970	0.87		
	2.776	2.826	2.850	2.817	14.730	0.19	6.23	44500	7140	0.89		
	2.800	2.850	2.800	2.817	14.630	0.19	6.23	44800	7190	0.90	7170	160
	2.800	2.800	2.750	2.783	14.850	0.19	6.08	38600*	6340*	0.79*		
	2.775	2.800	2.850	2.808	14.780	0.19	6.19	45600	7360	0.92		
1F	2.850	2.850	2.825	2.842	17.630	0.16	6.34	38800*	6120*	0.77*		
	2.800	2.850	2.825	2.825	17.600	0.16	6.27	44800	7150	0.90		
1G	2.750	2.800	2.825	2.792	12.780	0.22	6.12	44500	7270	0.91		
1H	2.800	2.850	2.776	2.808	12.180	0.23	6.19	44100	7120	0.89		
1J	2.850	2.825	2.800	2.825	10.730	0.26	6.27	46100	7360	0.92		
1K	2.750	2.825	2.800	2.792	10.360	0.27	6.12	46500	7600	0.95		
1L	2.800	2.825	2.850	2.825	9.760	0.29	6.27	45300	7390	0.93		

3 in. x 6 in. Standard Sulfur-Capped Cylinders, Paper Molds.

1						48600*	6870*	
2						54400	7690	
3			3.000		7.07	55000	7780	7800 140
4						56600	8010	
5						55600	7860	
6						54200	7670	

* Isperiectly capped.

Table 82 : Cylinder Set #2 : Sulfur-Capped (with TFE), PVC Molds.
Normal-weight aggregate.

Specimen I.D.	Specimen Dimensions					O/H	Area, sq. in.	Ult. Load, P, lb.	f=P/A	f'/f'c	Mean psi	Std. Dev. psi
	Dia.,01	Dia.,02	Dia.,03	Avg Dia.,0	Weight,N							
2S	2.825	2.850	2.775	2.817	3.56	0.79	6.23	47600	7640	1.03	7480	210
	2.850	2.850	2.800	2.833	3.38	0.84	6.30	45800	7260	0.97		
	2.775	2.850	2.825	2.817	3.34	0.84	6.23	48500	7780	1.04		
	2.775	2.800	2.850	2.808	3.39	0.83	6.19	46000	7430	1.00		
	2.850	2.800	2.775	2.808	3.42	0.82	6.19	45000	7270	0.98		
	2.850	2.825	2.850	2.842	3.36	0.85	6.34	47600	7510	1.01		
2S	2.850	2.776	2.800	2.808	6.24	0.45	6.19	47200	7620	1.02	7450	230
	2.800	2.850	2.825	2.825	6.33	0.46	6.27	47500	7580	1.02		
	2.775	2.850	2.800	2.808	6.21	0.46	6.19	47400	7650	1.03		
	2.800	2.825	2.850	2.825	6.22	0.45	6.27	46400	7400	0.99		
	2.850	2.825	2.800	2.825	6.32	0.46	6.27	44200	7050	0.95		
	2.775	2.825	2.800	2.800	6.23	0.45	6.16	45400	7370	0.99		
2C	2.875	2.800	2.850	2.842	9.11	0.31	6.34	44600	7030	0.94	7010	110
	2.800	2.875	2.850	2.842	9.11	0.31	6.34	44200	6970	0.94		
	2.850	2.800	2.825	2.825	9.16	0.31	6.27	43400	6920	0.93		
	2.800	2.850	2.825	2.825	9.28	0.30	6.27	45200	7210	0.97		
	2.825	2.875	2.850	2.850	9.18	0.31	6.38	44800	7020	0.94		
	2.825	2.775	2.850	2.817	9.26	0.30	6.23	43000	6900	0.93		
2C	2.775	2.850	2.800	2.808	11.83	0.24	6.19	44700	7220	0.97	6920	230
	2.825	2.875	2.850	2.850	11.82	0.24	6.38	44500	6980	0.94		
	2.776	2.825	2.850	2.817	11.93	0.24	6.23	44000	7060	0.96		
	2.775	2.850	2.800	2.808	11.91	0.24	6.19	42300	6830	0.92		
	2.800	2.825	2.850	2.825	11.96	0.24	6.27	41000	6540	0.88		
	2.800	2.850	2.825	2.826	12.02	0.24	6.27	43000	6860	0.92		
2E	2.775	2.800	2.825	2.800	14.90	0.19	6.16	41300	6710	0.90	6850	180
	2.800	2.825	2.850	2.825	14.86	0.19	6.27	43400	6920	0.93		
	2.850	2.825	2.800	2.825	14.78	0.19	6.27	44000	7020	0.94		
	2.800	2.850	2.825	2.825	14.86	0.19	6.27	44000	7020	0.94		
	2.825	2.850	2.775	2.817	14.92	0.19	6.23	41000	6580	0.88		
	2.800	2.825	2.850	2.825	14.73	0.19	6.27	42900	6840	0.92		
2F	2.775	2.850	2.825	2.817	17.64	0.16	6.23	39400	6320	0.85	6540	300
	2.775	2.800	2.825	2.800	17.50	0.16	6.16	38800	6300	0.85		
	2.825	2.800	2.850	2.825	17.48	0.16	6.27	39800	6350	0.85		
	2.775	2.800	2.825	2.800	17.48	0.16	6.16	43600	7080	0.95		
	2.775	2.825	2.800	2.800	17.66	0.16	6.16	40600	6590	0.88		
	2.775	2.825	2.850	2.817	17.63	0.16	6.23	41000	6580	0.88		

3 in. x 6 in. Standard Sulfur-Capped Cylinders, Paper Molds.

1								46800	6620		
2								45700	6460		
3				3.000			7.07	47900	6780	6670	170
4								47300	6690		
5								46100	6520		
6								49000	6930		

Table 83 : Cylinder Set #3 : Sulfur-Capped (without residual oil), PVC Molds.
Norsal-weight aggregate.

Specimen I.D.	Specimen Dimensions,in.					D/H	Area, sq. in.	Ult. Load, P,lb.	f'=P/A psi	f'/fc	Mean psi	Std. Dev. psi
	Dia.,D1	Dia.,D2	Dia.,D3	Avg Dia.,D	Height,H							
3a	2.776	2.825	2.850	2.817	3.28	0.86	6.23	56800	9120	1.15		
	2.800	2.850	2.876	2.842	3.62	0.81	6.34	52400e	8260e	1.04e		
	2.875	2.850	2.800	2.842	3.26	0.85	6.34	57800	9110	1.15	8880	210
	2.825	2.850	2.875	2.850	3.35	0.85	6.38	55800	8750	1.10		
	2.850	2.875	2.825	2.850	3.24	0.85	6.38	56600	8720	1.10		
	2.825	2.875	2.850	2.850	3.26	0.85	6.38	55600	8720	1.10		
3B	2.850	2.800	2.875	2.842	6.28	0.48	6.34	49400	7790	0.98		
	2.850	2.800	2.776	2.808	6.18	0.48	6.19	50900	8220	1.04	fc=	
	2.800	2.850	2.825	2.825	6.14	0.46	6.27	51300	8180	1.03	7940	320
	2.850	2.800	2.825	2.825	6.28	0.45	6.27	47300	7550	0.95		
	2.776	2.825	2.850	2.817	6.26	0.48	6.23	51400	8250	1.04		
	2.800	2.850	2.776	2.808	6.27	0.46	6.19	47200	7620	0.96		
3C	2.775	2.850	2.825	2.817	9.00	0.31	6.23	47600	7640	0.96		
	2.850	2.825	2.775	2.817	9.06	0.31	6.23	48000	7700	0.97		
	2.775	2.850	2.825	2.817	8.96	0.31	6.23	47600	7640	0.96	7590	200
	2.875	2.850	2.825	2.850	9.00	0.32	6.38	45900	7200	0.91		
	2.825	2.775	2.850	2.817	9.08	0.31	6.23	48400	7770	0.98		
	2.775	2.825	2.850	2.817	9.06	0.31	6.23	47200	7580	0.96		
3D	2.775	2.850	2.876	2.833	11.95	0.24	6.30	47500	7530	0.95		
	2.850	2.825	2.775	2.817	12.10	0.23	6.23	46600	7480	0.94		
	2.776	2.850	2.825	2.817	12.06	0.23	6.23	46300	7430	0.94	7500	40
	2.825	2.775	2.850	2.817	11.94	0.24	6.23	47000	7540	0.95		
	2.800	2.825	2.800	2.808	12.00	0.23	6.19	46400	7490	0.94		
	2.800	2.775	2.850	2.808	11.98	0.23	6.19	46800	7520	0.95		
3E	2.850	2.775	2.825	2.817	14.86	0.19	6.23	45900	7370	0.93		
	2.800	2.825	2.850	2.825	14.82	0.19	6.27	47400	7560	0.95		
	2.775	2.850	2.825	2.817	14.76	0.19	6.23	46400	7450	0.94	7410	80
	2.776	2.825	2.850	2.817	14.88	0.19	6.23	45800	7350	0.93		
	2.800	2.775	2.825	2.800	14.95	0.19	6.16	45200	7340	0.93		
	2.775	2.800	2.825	2.800	14.96	0.19	6.16	45600	7410	0.93		
3F	2.776	2.850	2.825	2.817	17.18	0.16	6.23	44500	7140	0.90		
	2.826	2.850	2.775	2.817	17.20	0.16	6.23	43000	6900	0.87		
	2.775	2.800	2.850	2.808	17.15	0.16	6.19	41600	6720	0.85	7020	180
	2.775	2.850	2.825	2.817	17.17	0.16	6.23	44000	7060	0.89		
	2.800	2.775	2.825	2.800	17.20	0.16	6.16	43600	7080	0.89		
	2.776	2.825	2.850	2.817	17.18	0.16	6.23	45000	7220	0.91		
3 in. e 6 in. Standard Sulfur-Capped Cylinders, Paper Molds.												
1								51200	7240			
2								52000	7360			
3				3.000			7.07	51900	7340		7280	130
4								52100	7370			
5			0					51800	7330			
6								49600	7020			

e Imperfectly capped.

Table A4 : Cylinder Set #4 : Ground Surface (without TFE), PVC Molds.
Norsel-weight aggregate.

Specimen I.D.	Specimen Dimensions, in.					D/H	Area, eq. in.	Ult. Load, P,lb.	f=P/A psi	f/fc	Mean psi	Std. Dev. psi
	Dia.,D1	Dia.,D2	Dia.,D3	Avg Dia.,D	Height,H							
4B	2.800	2.850	2.825	2.825	2.85	0.99	6.27	52400	8360	1.19		
	2.875	2.850	2.800	2.842	2.86	0.99	6.34	53400	8420	1.20		
	2.875	2.800	2.850	2.842	2.90	0.98	6.34	52600	8290	1.18	8390	60
	2.850	2.875	2.800	2.842	2.90	0.98	6.34	53400	8420	1.20		
	2.800	2.825	2.850	2.825	2.87	0.98	6.27	53000	8460	1.21		
	2.875	2.850	2.825	2.850	2.87	0.99	6.38	53600	8400	1.20		
4B	2.800	2.825	2.850	2.825	5.78	0.49	6.27	42800	6830	0.97		
	2.850	2.825	2.800	2.825	5.74	0.49	6.27	45700	7290	1.04		
	2.825	2.850	2.825	2.833	5.86	0.48	6.30	45000	7140	1.02	fc	
	2.775	2.825	2.850	2.817	5.71	0.49	6.23	43000	6900	0.98	7020	170
	2.775	2.800	2.850	2.808	5.72	0.49	6.19	42800	6910	0.98		
	2.800	2.850	2.825	2.825	5.86	0.48	6.27	44200	7050	1.00		
4C	2.800	2.825	2.850	2.825	8.68	0.33	6.27	41000	6540	0.93		
	2.850	2.825	2.875	2.850	8.61	0.33	6.38	43400	6800	0.97		
	2.850	2.800	2.825	2.825	8.56	0.33	6.27	43100	6880	0.98	6710	160
	2.875	2.850	2.800	2.842	8.61	0.33	6.34	43200	6810	0.97		
	2.875	2.800	2.850	2.842	8.59	0.33	6.34	41100	6480	0.92		
	2.800	2.825	2.850	2.825	8.58	0.33	6.27	42200	6730	0.96		
4D	2.825	2.800	2.850	2.825	11.44	0.25	6.27	39700	6330	0.90		
	2.825	2.850	2.875	2.850	11.47	0.25	6.38	40800	6400	0.91		
	2.850	2.775	2.825	2.817	11.44	0.25	6.23	40600	6520	0.93	6580	190
	2.825	2.875	2.850	2.850	11.51	0.25	6.38	43200	6770	0.96		
	2.800	2.825	2.875	2.833	11.56	0.25	6.30	42800	6790	0.97		
	2.800	2.825	2.850	2.825	11.45	0.25	6.27	41600	6640	0.95		
4E	2.800	2.875	2.850	2.842	14.38	0.20	6.34	40300	6350	0.90		
	2.800	2.825	2.875	2.833	14.36	0.20	6.30	42000	6660	0.95		
	2.875	2.850	2.800	2.842	14.37	0.20	6.34	41200	6500	0.93	6450	120
	2.775	2.825	2.850	2.817	14.41	0.20	6.23	39700	6370	0.91		
	2.800	2.825	2.850	2.825	14.33	0.20	6.27	40500	6460	0.92		
	2.800	2.825	2.850	2.825	14.38	0.20	6.27	39800	6350	0.90		
4F	2.775	2.825	2.800	2.800	17.21	0.16	6.16	40000	6500	0.93		
	2.800	2.850	2.825	2.825	17.23	0.16	6.27	39600	6320	0.90		
	2.775	2.850	2.825	2.817	17.24	0.16	6.23	39700	6370	0.91	6420	90
	2.800	2.825	2.800	2.808	17.21	0.16	6.19	40500	6540	0.93		
	2.800	2.825	2.850	2.825	17.18	0.16	6.27	39800	6350	0.90		
	2.825	2.775	2.800	2.800	17.22	0.16	6.16	39600	6430	0.92		

3 in. x 6 in. Standard Sulfur-Capped Cylinders, Paper Molds.

1								44000	6220			
2								42000	5940			
3				3.000			7.07	45700	6460		6260	190
4								44100	6240			
5								45500	6440			
6								44100	6240			

Table A5 : Cylinder Set #5 : Ground Surface (with TFE), PVC Molds.
Basal-weight aggregate.

Specimen I.D.	Specimen Diameters,in.					O/H	Area, sq. in.	Ult. Load, P,lb.	f=P/A psi	f/fc	Mean psi	Std. Dev. psi
	Dia.,01	Dia.,02	Dia.,03	Avg Dia.,D	Height,H							
5B	2.850	2.825	2.800	2.825	2.91	0.97	6.28	52000	8290	1.09		
	2.775	2.825	2.850	2.817	2.88	0.98	6.24	52300	8380	1.10		
	2.775	2.825	2.850	2.817	2.88	0.98	6.24	51200	8210	1.08	8070	150
	2.775	2.850	2.825	2.817	2.95	0.95	6.24	49600	7950	1.05		
	2.800	2.875	2.825	2.833	2.93	0.97	6.31	51100	8090	1.07		
	2.850	2.775	2.825	2.817	2.91	0.97	6.24	50600	8110	1.07		
5A	2.800	2.850	2.875	2.842	6.86	0.48	6.34	47800	7540	0.99		
	2.775	2.825	2.850	2.817	6.83	0.48	6.23	47900	8010	1.06		
	2.775	2.850	2.825	2.817	6.76	0.49	6.23	47500	7620	1.00	fc	
	2.800	2.825	2.875	2.833	6.73	0.49	6.30	46000	7300	0.96	7590	300
	2.850	2.800	2.825	2.825	6.83	0.48	6.27	45200	7850	1.03		
	2.850	2.875	2.825	2.850	6.82	0.49	6.38	46200	7240	0.95		
5C	2.850	2.800	2.775	2.808	8.75	0.32	6.19	47100	7600	1.00		
	2.825	2.875	2.850	2.850	8.74	0.33	6.28	46600	7300	0.96		
	2.825	2.800	2.875	2.833	8.74	0.32	6.30	43200	6850	0.90	7250	270
	2.875	2.825	2.800	2.833	8.58	0.32	6.30	46000	7300	0.96		
	2.800	2.850	2.825	2.825	8.66	0.33	6.27	44000	7020	0.92		
	2.825	2.875	2.850	2.850	8.66	0.33	6.38	47400	7430	0.98		
5D	2.800	2.850	2.825	2.826	11.54	0.24	6.27	46000	7240	0.97		
	2.875	2.850	2.800	2.842	11.54	0.25	6.24	44600	7030	0.93		
	2.800	2.875	2.850	2.842	11.56	0.25	6.24	43100	6800	0.90	7050	190
	2.775	2.825	2.850	2.817	11.56	0.24	6.23	44300	7110	0.94		
	2.875	2.825	2.850	2.850	11.56	0.25	6.28	45200	7090	0.93		
	2.875	2.850	2.825	2.850	11.58	0.25	6.38	44000	6900	0.91		
5E	2.825	2.850	2.875	2.850	14.44	0.20	6.38	45000	7050	0.93		
	2.875	2.850	2.825	2.850	14.40	0.20	6.28	42000	6580	0.87		
	2.775	2.850	2.800	2.808	14.37	0.20	6.19	45900	7410	0.98	7080	330
	2.775	2.850	2.825	2.817	14.41	0.20	6.23	44600	7160	0.94		
	2.800	2.825	2.850	2.825	14.44	0.20	6.27	46500	7420	0.98		
	2.800	2.825	2.850	2.825	14.46	0.20	6.27	43000	6860	0.90		
5F	2.850	2.800	2.775	2.808	17.29	0.16	6.19	43800	7070	0.93		
	2.775	2.800	2.850	2.808	17.28	0.16	6.19	45400	7330	0.97		
	2.825	2.850	2.775	2.817	17.21	0.16	6.23	43600	7000	0.92	7040	240
	2.775	2.850	2.825	2.817	17.26	0.16	6.23	45400	7290	0.96		
	2.825	2.850	2.875	2.850	17.34	0.16	6.28	43300	6790	0.89		
	2.875	2.850	2.800	2.842	17.28	0.16	6.34	43000	6780	0.89		

3 in. x 6 in. Standard Sulfur-Capped Cylinders, Paper Molds.

1								46200	6540			
2								48000	6790			
3				3.000			7.07	50000	7070		6750	190
4								46600	6590			
5								48100	6800			
6								47600	6730			

Table AG : Cylinder Set #6 : Standard Sulfur-Capped (with residual oil), PVC Molds.
Light-weight aggregate.

Specimen I.D.	Specimen Dimensions,in.					D/H	Area sq. in.	Ult. Load, P,lb.	f=P/A psi	f/fc	Mean psi	Std. Dev. psi
	Dia.,D1	Dia.,D2	Dia.,D3	Avg Dia.,D	Height,H							
6A	2.825	2.875	2.850	2.850	3.30	0.86	6.38	40000	6270	0.99		
	2.800	2.850	2.875	2.842	3.23	0.88	6.34	40200	6340	1.00		
	2.775	2.875	2.850	2.833	3.25	0.87	6.30	41800	6630	1.05	6370	140
	2.800	2.850	2.875	2.842	3.26	0.87	6.34	40800	6430	1.01		
	2.850	2.800	2.875	2.842	3.60	0.84	6.34	39600	6240	0.98		
	2.875	2.850	2.775	2.833	3.33	0.85	6.30	39800	6310	1.00		
6B	2.800	2.825	2.875	2.833	6.18	0.46	6.30	40400	6410	1.01		
	2.800	2.825	2.850	2.825	6.22	0.45	6.27	39800	6350	1.00		
	2.800	2.825	2.850	2.825	6.20	0.46	6.27	39000	6220	0.98	fc	
	2.850	2.825	2.800	2.825	6.23	0.45	6.27	39000	6220	0.98	6340	160
	2.825	2.850	2.800	2.825	6.22	0.45	6.27	39000	6220	0.98		
	2.775	2.800	2.825	2.800	6.23	0.45	6.16	40700	6610	1.04		
6C	2.800	2.825	2.850	2.825	9.00	0.31	6.27	39500	6300	0.99		
	2.825	2.875	2.850	2.850	8.97	0.32	6.38	38000	5960	0.94		
	2.825	2.850	2.875	2.850	9.02	0.32	6.38	38800	6080	0.96	6100	140
	2.775	2.850	2.875	2.833	8.98	0.32	6.30	35000*	5550*	0.88*		
	2.800	2.850	2.875	2.842	8.93	0.32	6.34	38000	5990	0.94		
	2.775	2.850	2.825	2.817	8.96	0.31	6.23	38500	6180	0.97		
6D	2.800	2.825	2.850	2.825	11.89	0.24	6.27	37000	5900	0.93		
	2.775	2.825	2.850	2.817	11.90	0.24	6.23	37600	6030	0.95		
	2.775	2.850	2.800	2.808	11.81	0.24	6.19	35400	5720	0.90	5850	120
	2.800	2.875	2.850	2.842	11.88	0.24	6.34	29600	4670	0.74		
	2.825	2.800	2.850	2.825	11.93	0.24	6.27	36400	5810	0.92		
	2.800	2.850	2.825	2.825	11.83	0.24	6.27	36400	5810	0.92		
6E	2.825	2.850	2.875	2.850	14.83	0.19	6.38	38400	6020	0.95		
	2.850	2.800	2.775	2.808	14.73	0.19	6.19	35400	5720	0.90		
	2.850	2.800	2.825	2.825	14.84	0.19	6.27	35900	5730	0.90	5710	220
	2.800	2.875	2.825	2.833	14.74	0.19	6.30	35400	5620	0.89		
	2.825	2.775	2.800	2.800	14.76	0.19	6.16	33000	5360	0.85		
	2.775	2.850	2.825	2.817	14.78	0.19	6.23	36000	5780	0.91		
6F	2.775	2.850	2.875	2.833	17.15	0.17	6.30	35100	5570	0.88		
	2.800	2.875	2.825	2.833	17.14	0.17	6.30	34400	5460	0.86		
	2.775	2.850	2.800	2.808	17.23	0.16	6.19	36400	5880	0.93	5640	170
	2.775	2.825	2.850	2.817	17.15	0.16	6.23	34200	5490	0.87		
	2.875	2.775	2.825	2.825	17.10	0.17	6.27	36400	5810	0.92		
	2.775	2.850	2.825	2.817	17.25	0.16	6.23	35100	5630	0.89		

3 in. x 6 in. Standard Sulfur-Capped Cylinders,Paper Molds

1								38200	5400			
2								39400	5570			
3				3.000			7.07	38100	5390		5550	140
4								39100	5530			
5								40000	5660			
6								40600	5740			

* Imperfectly capped

Table A7: Comparision of Ultimate Stress in Cylinders of Diameter to Height Ratio of 1.00 and 0.50. Light-weight concrete, Paper Molds.

Specimen I.D.	D/H	Area, sq. in.	Ult. Load, P,lb.	Area, psi	Mean, psi	Std. Dev. psi
1			40200	5690		
2			38200	5400		
3			40400	5710		
4			37000	5230		
5	1.00	7.07	39600	5600	5580	200
6			38600	5460		
7			38600	5460		
8			40700	5760		
9			41500	5870		
1			37500	5300		
2			39800	5630		
3			37800	5350		
4			39000	5520		
5	0.50	7.07	39000	5520	5510	190
6			40400	5710		
7			41200	5830		
8			38200	5400		
9			37400	5290		

Table A8: Cylinder Stress-Strain Data.
Standard Sulfur-Capped (without residual oil), PVC Molds.
H = 3.36 in., D = 2.85 in., D/H = 0.85, Area = 6.38 sq. in.

Load, lb.	Stress,P/A psi	Lateral Strain, Microstrain			Axial Strain, Microstrain		
		Gage 1	Gage 2	Average	Gage 1	Gage 2	Average
0	0	0	0	0	0	*	0
3000	470	2	27	15	-99		-99
5200	820	5	44	25	-139		-139
10000	1570	16	86	51	-264		-264
15600	2450	40	135	88	-450		-450
20200	3170	64	172	118	-595		-595
25600	4010	101	222	162	-774		-774
30400	4760	133	263	198	-913		-913
35600	5580	182	324	253	-1076		-1076
40800	6390	241	392	317	-1248		-1248
45000	7050	312	476	394	-1495		-1495
49800	7810	442	675	559	-1886		-1886
51000	7990	505	800	653	-1981		-1981
52400	8210	570	973	772			
54500	8540	712	1680	1196			
55600	8720	1288	> Range	1288			

* Only one axial Strain Gage was mounted.

Table A9: Cylinder Stress-Strain Data.
Standard Sulfur-Capped (without residual oil), PVC Molds.
H = 6.27 in., D = 2.81 in., D/H = 0.45, Area = 6.19 sq. in.

Load, lb.	Stress, P/A psi	Lateral Strain, Microstrain			Axial Strain, Microstrain		
		Gage 1	Gage 2	Average	Gage 1	Gage 2	Average
0	0	0	0	*	0	0	0
3000	480	60	-13		-53	-115	-84
5000	810	83	-13		-124	-152	-138
10000	1620	144	2		-300	-281	-291
15200	2460	201	28		-494	-450	-472
20000	3230	254	53		-652	-602	-627
25000	4040	319	87		-842	-790	-816
30000	4850	403	124		-1045	-975	-1010
35000	5650	540	168		-1291	-1210	-1251
40000	6460	767	222		-1582	-1431	-1507
44600	7210	1489	329		-2012	-1747	-1880
46000	7430	2258	451		-2286	-1947	-2117
47200	7620	> Range	815		-2852	-2147	-2500

* Strain Gage 2 malfunctioned.

Table A10: Cylinder Stress-Strain Data.
Standard Sulfur-Capped (without residual oil), PVC Molds.
H = 9.06 in., D = 2.82 in., D/H = 0.31, Area = 6.23 sq. in.

Load, lb.	Stress, P/A psi	Lateral Strain, Microstrain			Axial Strain, Microstrain		
		Gage 1	Gage 2	Average	Gage 1	Gage 2	Average
0	0	0	0	0	0	0	0
3000	480	13	27	20	-74	-103	-89
5000	800	22	44	33	-111	-168	-140
10000	1610	45	94	70	-229	-341	-285
15000	2410	77	149	113	-368	-525	-447
20000	3210	111	201	156	-519	-704	-612
25000	4010	152	268	210	-701	-903	-802
30000	4820	191	341	266	-873	-1095	-984
35000	5620	249	464	357	-1092	-1338	-1215
40000	6420	333	690	512	-1379	-1656	-1518
43200	6930	408	856	632	-1562	-1849	-1706
45000	7220	478	991	735	-1695	-1964	-1830
46000	7380	579	1168	874	-1823	-2063	-1943
47200	7580	954	1665	1310	-2010	-2067	-2039

Table A11: Cylinder Stress-Strain Data.
Standard Sulfur-Capped (without resuidual oil), PVC Molds.
H = 11.98 in., D = 2.81 in., D/H = 0.23, Area = 6.19 sq. in.

Load, lb.	Stress,P/A psi	Lateral Strain, Microstrain			Axial Strain, Microstrain		
		Gage 1	Gage 2	Average	Gage 1	Gage 2	Average
0	0	0	0	0	0	0	0
3400	550	28	21	25	-101	-112	-107
5600	900	47	30	39	-145	-200	-173
8000	1290	68	42	55	-193	-280	-237
10000	1620	84	51	68	-246	-355	-301
15000	2420	128	83	106	-387	-537	-462
20000	3230	169	115	142	-536	-714	-625
25000	4040	216	158	187	-710	-914	-812
30000	4850	265	202	234	-886	-1110	-998
35000	5650	331	261	296	-1091	-1340	-1216
40000	6460	417	345	381	-1326	-1620	-1473
43000	6950	495	419	457	-1492	-1836	-1664
45000	7270	575	506	541	-1630	-2025	-1828
46000	7430	705	640	673	-1743	-2241	-1992
46600	7520						

Table A12: Cylinder Stress-Strain Data.
Standard Sulfur-Capped (without residual oil), PVC Molds.
H = 14.96 in., D = 2.82 in., D/H = 0.19, Area = 6.16 sq. in.

Load, lb.	Stress, P/A psi	Lateral Strain, Microstrain			Axial Strain, Microstrain		
		Gage 1	Gage 2	Average	Gage 1	Gage 2	Average
0	0	0	0	0	0	0	0
5000	810	36	29	33	-132	-172	-152
8000	1300	48	56	52	-216	-260	-238
10000	1620	61	75	68	-297	-341	-319
13200	2140	80	104	92	-403	-452	-428
15000	2440	92	119	106	-465	-517	-491
20000	3250	126	171	149	-633	-691	-662
25000	4060	166	230	198	-826	-894	-860
30000	4870	209	305	257	-1021	-1099	-1060
35000	5680	266	413	340	-1250	-1342	-1296
40000	6490	345	596	471	-1542	-1643	-1593
41000	6660	378	692	535	-1674	-1765	-1720
42000	6820	404	780	592	-1777	-1861	-1819
45000	7310	481	1165	823	-2195	-2150	-2173
45600	7410						

Table A13: Cylinder Stress-Strain Data.
Standard Sulfur-Capped (without residual oil), PVC Molds.
H = 17.18 in., D = 2.82 in., D/H = 0.16, Area = 6.23 sq.in.

Load, lb.	Stress, P/A psi	Lateral Strain, Microstrain			Axial Strain, Microstrain		
		Gage 1	Gage 2	Average	Gage 1	Gage 2	Average
0	0	0	0	0	0	0	0
3000	480	22	23	23	-117	-82	-100
5000	800	29	38	34	-161	-150	-156
8000	1280	44	59	52	-248	-236	-242
10000	1610	58	74	66	-317	-315	-316
12800	2050	79	96	88	-406	-417	-412
14600	2340	90	107	99	-462	-484	-473
17400	2790	112	129	121	-550	-585	-568
19600	3150	127	142	135	-623	-669	-646
23000	3690	152	168	160	-731	-798	-765
25000	4010	170	181	176	-807	-887	-847
28000	4490	195	208	202	-911	-1009	-960
30000	4820	215	224	220	-994	-1108	-1051
35000	5620	271	276	274	-1196	-1343	-1270
40000	6420	367	352	360	-1493	-1692	-1590
45000	7220	529	534	532	-1993	-2170	-2080

Table A14: Cylinder Stress-Strain Data.
Standard Sulfur-Capped (without residual oil), Paper Molds.
3 in. x 6 in. Standard Cylinder, Area = 7.07 sq. in.

Load, lb.	Stress, P/A psi	Lateral Strain, Microstrain			Axial Strain, Microstrain		
		Gage 1	Gage 2	Average	Gage 1	Gage 2	Average
0	0	0	0	0	0	0	0
3000	420	20	6	13	-112	-63	-88
5000	710	32	13	23	-162	-158	-160
10000	1410	64	40	52	-301	-240	-271
15200	2150	97	74	86	-461	-385	-423
20000	2830	132	105	119	-614	-518	-566
25400	3590	172	146	159	-790	-683	-737
30200	4270	214	192	203	-962	-855	-909
36000	5090	273	257	265	-1175	-1066	-1121
40800	5770	338	337	338	-1419	-1281	-1350
45000	6360	417	417	417	-1699	-1491	-1595
46200	6530	547	517	532	-1958	-1652	-1805
47200	6680	642	601	622	-2138	-1764	-1951
48600	6870	835	759	797	-2449	-1925	-2187
49600	7020						

Table A15: Load-Stress Data, Beam B1, Normal-weight aggregate.

Major Thrust, P1, lb.	Minor Thrust, P2, lb.	Strain at Comp. Face, Microstrain			f	n	df/dε	dn/dε	fc = ε(df/dε)+f	fc = ε(dn/dε) + 2n	Average fc
		Gage 1	Gage 2	Average							
0	0	0	0	0	0	0	3.73	2.75	0	0	0
6000	160	-44	-42	-43	246	155	3.68	2.70	405	425	410
10000	340	-105	-112	-109	414	273	3.60	2.61	807	832	820
15000	470	-156	-167	-162	619	402	3.54	2.55	1193	1215	1200
20000	600	-207	-227	-217	824	530	3.48	2.47	1579	1596	1590
25000	750	-266	-295	-281	1030	662	3.40	2.39	1986	1996	1990
30000	910	-327	-366	-347	1236	797	3.33	2.31	2391	2393	2390
35000	1060	-384	-434	-409	1442	929	3.25	2.23	2773	2768	2770
40000	1250	-447	-507	-477	1650	1070	3.17	2.14	3164	3160	3160
45000	1420	-514	-584	-549	1857	1207	3.09	2.04	3553	3536	3540
50000	1580	-574	-657	-616	2063	1341	3.01	1.96	3918	3889	3900
55000	1740	-639	-735	-687	2270	1476	2.93	1.87	4281	4234	4260
60000	1880	-701	-812	-757	2475	1606	2.85	1.78	4630	4556	4590
65000	2040	-768	-894	-831	2682	1741	2.76	1.68	4975	4877	4930
70000	2190	-824	-966	-895	2888	1873	2.68	1.60	5290	5175	5230
75000	2330	-895	-1053	-974	3093	2003	2.59	1.49	5618	5462	5540
80000	2450	-960	-1139	-1050	3298	2129	2.50	1.40	5926	5725	5830
85000	2570	-1020	-1224	-1122	3503	2255	2.42	1.30	6217	5972	6090
90000	2690	-1086	-1318	-1202	3708	2381	2.33	1.20	6503	6204	6350
95000	2800	-1156	-1422	-1289	3912	2505	2.22	1.09	6778	6411	6590
100000	2870	-1228	-1536	-1382	4115	2620	2.11	0.97	7037	6576	6810
105000	2980	-1307	-1670	-1489	4319	2744	1.99	0.83	7281	6721	7000
110000	3060	-1399	-1822	-1611	4522	2861	1.85	0.67	7497	6802	7150
115000	3100	-1481	-1966	-1724	4724	2970	1.71	0.52	7679	6843	7260
120000		-1587	-2088	-1838	4800	2400					

Table A16: Computation of df/dϵ, Beam B1.

x(= ϵ)	y (= f)	x*x	x*x*x	x*x*x*x	x*y	x*x*y	Pred. y	Residuals
0	0	0	0.000E+00	0.000E+00	0.000E+00	0.000E+00	20	20
43	246	1849	7.951E+04	3.419E+06	1.058E+04	4.549E+05	180	-66
109	414	11881	1.295E+06	1.412E+08	4.513E+04	4.919E+06	420	6
162	619	26244	4.252E+06	6.887E+08	1.003E+05	1.625E+07	609	-10
217	824	47089	1.022E+07	2.217E+09	1.788E+05	3.880E+07	803	-21
281	1030	78961	2.219E+07	6.235E+09	2.894E+05	8.133E+07	1023	-7
347	1236	120409	4.178E+07	1.450E+10	4.289E+05	1.488E+08	1245	9
409	1442	167281	6.842E+07	2.798E+10	5.898E+05	2.412E+08	1449	7
477	1650	227529	1.085E+08	5.177E+10	7.871E+05	3.754E+08	1667	17
549	1857	301401	1.655E+08	9.084E+10	1.019E+06	5.597E+08	1893	36
616	2063	379456	2.337E+08	1.440E+11	1.271E+06	7.828E+08	2097	34
687	2270	471969	3.242E+08	2.228E+11	1.559E+06	1.071E+09	2308	38
757	2475	573049	4.338E+08	3.284E+11	1.874E+06	1.418E+09	2510	35
831	2682	690561	5.739E+08	4.769E+11	2.229E+06	1.852E+09	2718	36
895	2888	801025	7.169E+08	6.416E+11	2.585E+06	2.313E+09	2892	4
974	3093	948676	9.240E+08	9.000E+11	3.013E+06	2.934E+09	3100	7
1050	3298	1102500	1.158E+09	1.216E+12	3.463E+06	3.636E+09	3294	-4
1122	3503	1258884	1.412E+09	1.585E+12	3.930E+06	4.410E+09	3471	-32
1202	3708	1444804	1.737E+09	2.087E+12	4.457E+06	5.357E+09	3661	-47
1289	3912	1661521	2.142E+09	2.761E+12	5.043E+06	6.500E+09	3859	-53
1382	4115	1909924	2.640E+09	3.648E+12	5.687E+06	7.859E+09	4060	-55
1489	4319	2217121	3.301E+09	4.916E+12	6.431E+06	9.576E+09	4280	-39
1611	4522	2595321	4.181E+09	6.736E+12	7.285E+06	1.174E+10	4514	-8
1724	4724	2972176	5.124E+09	8.834E+12	8.144E+06	1.404E+10	4715	-9
1838	4800	3378244	6.209E+09	1.141E+13	8.822E+06	1.622E+10		
20061	61690	23386026	3.153E+10	4.61E+13	6.924E+07	9.117E+10		

Equation of curve of best fit to data set:
y = -5.85349E-04*x*x + 3.732411*x + 20.1667

Table A17: Computation of dm/dϵ, Beam B1.

x (= ϵ)	y (= f)	x*x	x*x*x	x*x*x*x	x*y	x*x*y	Pred. y	Residuals
0	0	0	0.000E+00	0.000E+00	0.000E+00	0.000E+00	-48	-48
43	155	1849	7.951E+04	3.419E+06	6.665E+03	2.866E+05	69	-86
109	273	11881	1.295E+06	1.412E+08	2.976E+04	3.244E+06	244	-29
162	402	26244	4.252E+06	6.887E+08	6.512E+04	1.055E+07	381	-21
217	530	47089	1.022E+07	2.217E+09	1.150E+05	2.496E+07	519	-11
281	662	78961	2.219E+07	6.235E+09	1.860E+05	5.227E+07	675	13
347	797	120409	4.178E+07	1.450E+10	2.766E+05	9.597E+07	830	33
409	929	167281	6.842E+07	2.798E+10	3.800E+05	1.554E+08	970	41
477	1070	227529	1.085E+08	5.177E+10	5.104E+05	2.435E+08	1119	49
549	1207	301401	1.655E+08	9.084E+10	6.626E+05	3.638E+08	1269	62
616	1341	379456	2.337E+08	1.440E+11	8.261E+05	5.089E+08	1403	62
687	1476	471969	3.242E+08	2.228E+11	1.014E+06	6.966E+08	1539	63
757	1606	573049	4.338E+08	3.284E+11	1.216E+06	9.203E+08	1666	60
831	1741	690561	5.739E+08	4.769E+11	1.447E+06	1.202E+09	1794	53
895	1873	801025	7.169E+08	6.416E+11	1.676E+06	1.500E+09	1899	26
974	2003	948676	9.240E+08	9.000E+11	1.951E+06	1.900E+09	2021	18
1050	2129	1102500	1.158E+09	1.216E+12	2.235E+06	2.347E+09	2131	2
1122	2255	1258884	1.412E+09	1.585E+12	2.530E+06	2.839E+09	2228	-27
1202	2381	1444804	1.737E+09	2.087E+12	2.862E+06	3.440E+09	2328	-53
1289	2505	1661521	2.142E+09	2.761E+12	3.229E+06	4.162E+09	2428	-77
1382	2620	1909924	2.640E+09	3.648E+12	3.621E+06	5.004E+09	2523	-97
1489	2744	2217121	3.301E+09	4.916E+12	4.086E+06	6.084E+09	2619	-125
1611	2861	2595321	4.181E+09	6.736E+12	4.609E+06	7.425E+09	2711	-150
1724	2970	2972176	5.124E+09	8.834E+12	5.120E+06	8.827E+09	2778	-192
1838	2400	3378244	6.209E+09	1.141E+13	4.411E+06	8.108E+09		
20061	38930	23387875	3.153E+10	4.610E+13	4.307E+07	5.591E+10		

Equation of curve of best fit to data set:
y = -6.468587E-04*x*x + 2.754722*x - 48.15308

Table A18: Cylinder Stress-Strain Data, Companion Cylinder to Beam B1.
3 in. x 6 in. Standard Sulfur-Capped, Paper Molds.
Area = 7.07 sq. in.

Load, P, lb.	Stress, psi	Axial Strain, Microstrain Gage 1	Gage 2	Average
0	0	0	0	0
5900	830	-179	-166	-173
10000	1410	-337	-237	-287
15200	2150	-503	-336	-420
20000	2830	-657	-462	-560
25000	3540	-811	-599	-705
30200	4270	-967	-747	-857
35000	4950	-1127	-901	-1014
40400	5710	-1310	-1088	-1199
45000	6360	-1499	-1282	-1391
47000	6650	-1598	-1400	-1499
49000	6930	-1694	-1520	-1607
50800	7190	-1802	-1667	-1735
53800	7610	-1966	-1948	-1957
51800	7330	-2174	-2090	-2132

Table A19: Load-Stress Data, Beam B2, Light-weight aggregate.

Major Thrust, P1, lb.	Minor Thrust, P2, lb.	Strain at Comp. Face, Microstrain			f	n	df/dε	da/dε	fc = ε(df/dε)+f	fc = ε(da/dε) + 2a	Average fc
		Gage 1	Gage 2	Average							
0	0	0	0	0	0	0	2.00	1.41	0	0	0
5500	190	109	98	104	228	151	1.99	1.39	433	446	440
10000	360	219	196	208	414	278	1.97	1.37	824	840	830
15000	520	329	295	312	621	412	1.96	1.35	1232	1245	1240
20000	680	437	396	417	827	547	1.95	1.32	1638	1645	1640
25000	870	564	517	541	1035	688	1.93	1.30	2079	2077	2080
30000	1000	667	614	641	1240	816	1.92	1.28	2470	2449	2460
35000	1160	785	726	756	1446	951	1.91	1.25	2886	2846	2870
40000	1330	906	845	876	1653	1087	1.89	1.22	3309	3247	3280
45000	1500	1030	974	1002	1860	1224	1.88	1.20	3740	3648	3690
50000	1650	1049	1097	1073	2066	1356	1.87	1.18	4070	3981	4030
55000	1800	1120	1225	1173	2272	1489	1.86	1.16	4447	4338	4390
60000	1940	1226	1358	1292	2478	1619	1.84	1.13	4856	4704	4780
62000	1990	1268	1419	1344	2560	1670	1.83	1.12	5024	4849	4940
64000	2040	1282	1473	1378	2642	1721	1.83	1.12	5163	4979	5070
66000	2090	1303	1526	1415	2724	1771	1.83	1.11	5306	5110	5210
68000	2130	1327	1580	1454	2805	1820	1.82	1.10	5452	5239	5350
70000	2190	1356	1636	1496	2888	1873	1.82	1.09	5604	5378	5490
72000	2230	1402	1688	1545	2969	1922	1.81	1.08	5766	5512	5640
74000	2280	1435	1745	1590	3051	1972	1.80	1.07	5920	5647	5780
76000	2310	1468	1801	1635	3132	2019	1.80	1.06	6073	5772	5920
78000	2350	1510	1860	1685	3214	2068	1.79	1.05	6235	5904	6070
80000	2400	1552	1918	1735	3296	2118	1.79	1.04	6396	6039	6220
82000	2450	1558	1979	1769	3378	2169	1.78	1.03	6531	6163	6350
84000	2480	1625	2038	1832	3459	2216	1.78	1.02	6710	6296	6500
86000	2500	1634	2106	1870	3540	2260	1.77	1.01	6851	6408	6630
88000	2530	1668	2158	1913	3621	2306	1.77	1.00	6998	6527	6760
90000	2560	1708	2228	1968	3702	2353	1.76	0.99	7163	6651	6910
92000	2570	1748	2248	1998	3783	2395	1.75	0.98	7289	6752	7020
94000	2590	1788	2308	2048	3864	2439	1.75	0.97	7445	6868	7160
96000	2590	1838	2378	2108	3944	2479	1.74	0.96	7615	6979	7300
98000	2580	1878	2458	2168	4023	2517	1.73	0.95	7783	7084	7430
100000	2550	1898	2528	2213	4102	2551	1.73	0.94	7928	7172	7550
102000	2510	1978	2658	2318	4180	2582	1.72	0.91	8158	7280	7720

Table A20: Computation of df/dθ, Beam B2.

x(= θ)	y (= f)	x*x	x*x*x	x*x*x*x	x*y	x*x*y	Pred. y	Residuals
0	0	0.000E+00	0.000E+00	0.000E+00	0.000E+00	0.000E+00	0	0
104	228	1.082E+04	1.125E+06	1.170E+08	2.371E+04	2.466E+06	207	-21
208	414	4.326E+04	8.999E+06	1.872E+09	8.611E+04	1.791E+07	413	-1
312	621	9.734E+04	3.037E+07	9.476E+09	1.938E+05	6.045E+07	617	-4
417	827	1.739E+05	7.251E+07	3.024E+10	3.449E+05	1.438E+08	822	-5
541	1035	2.927E+05	1.583E+08	8.566E+10	5.599E+05	3.029E+08	1063	28
641	1240	4.109E+05	2.634E+08	1.688E+11	7.948E+05	5.095E+08	1255	15
756	1446	5.715E+05	4.321E+08	3.267E+11	1.093E+06	8.264E+08	1475	29
876	1653	7.674E+05	6.722E+08	5.889E+11	1.448E+06	1.268E+09	1703	50
1002	1860	1.004E+06	1.006E+09	1.008E+12	1.864E+06	1.867E+09	1941	81
1073	2066	1.151E+06	1.235E+09	1.326E+12	2.217E+06	2.379E+09	2073	7
1173	2272	1.376E+06	1.614E+09	1.893E+12	2.665E+06	3.126E+09	2260	-12
1292	2478	1.669E+06	2.157E+09	2.786E+12	3.202E+06	4.136E+09	2480	2
1344	2560	1.806E+06	2.428E+09	3.263E+12	3.441E+06	4.624E+09	2575	15
1378	2642	1.899E+06	2.617E+09	3.606E+12	3.641E+06	5.017E+09	2637	-5
1415	2724	2.002E+06	2.833E+09	4.009E+12	3.854E+06	5.454E+09	2705	-19
1454	2805	2.114E+06	3.074E+09	4.469E+12	4.078E+06	5.930E+09	2776	-29
1496	2888	2.238E+06	3.348E+09	5.009E+12	4.320E+06	6.463E+09	2852	-36
1545	2969	2.387E+06	3.688E+09	5.698E+12	4.587E+06	7.087E+09	2941	-28
1590	3051	2.528E+06	4.020E+09	6.391E+12	4.851E+06	7.713E+09	3023	-28
1635	3132	2.673E+06	4.371E+09	7.146E+12	5.121E+06	8.373E+09	3104	-28
1685	3214	2.839E+06	4.784E+09	8.061E+12	5.416E+06	9.125E+09	3194	-20
1735	3296	3.010E+06	5.223E+09	9.061E+12	5.719E+06	9.922E+09	3283	-13
1769	3378	3.129E+06	5.536E+09	9.793E+12	5.976E+06	1.057E+10	3344	-34
1832	3459	3.356E+06	6.149E+09	1.126E+13	6.337E+06	1.161E+10	3456	-3
1870	3540	3.497E+06	6.539E+09	1.223E+13	6.620E+06	1.238E+10	3523	-17
1913	3621	3.660E+06	7.001E+09	1.339E+13	6.927E+06	1.325E+10	3599	-22
1968	3702	3.873E+06	7.622E+09	1.500E+13	7.286E+06	1.434E+10	3696	-6
1998	3783	3.992E+06	7.976E+09	1.594E+13	7.558E+06	1.510E+10	3749	-34
2048	3864	4.194E+06	8.590E+09	1.759E+13	7.913E+06	1.621E+10	3836	-28
2108	3944	4.444E+06	9.367E+09	1.975E+13	8.314E+06	1.753E+10	3941	-3
2168	4023	4.700E+06	1.019E+10	2.209E+13	8.722E+06	1.891E+10	4045	22
2213	4102	4.897E+06	1.084E+10	2.398E+13	9.078E+06	2.009E+10	4123	21
2318	4180	5.373E+06	1.245E+10	2.887E+13	9.689E+06	2.246E+10	4304	124
45877	87017	7.618E+07	1.363E+11	2.548E+14	1.439E+08	2.568E+11		

Equation of the curve of best fit to data set:
y = 6.075112E-05*x*x + 1.997719*x - 0.1280451

Table A21: Computation of dm/d6, Beam B2.

x(= 6)	y (= m)	x*x	x*x*x	x*x*x*x	x*y	x*x*y	Pred. y	Residuals
0	0	0.000E+00	0.000E+00	0.000E+00	0.000E+00	0.000E+00	-23	-23
104	151	1.082E+04	1.125E+06	1.170E+08	1.570E+04	1.633E+06	123	-28
208	278	4.326E+04	8.999E+06	1.872E+09	5.782E+04	1.203E+07	266	-12
312	412	9.734E+04	3.037E+07	9.476E+09	1.285E+05	4.011E+07	407	-5
417	547	1.739E+05	7.251E+07	3.024E+10	2.281E+05	9.512E+07	547	0
541	688	2.927E+05	1.583E+08	8.566E+10	3.722E+05	2.014E+08	710	22
641	816	4.109E+05	2.634E+08	1.688E+11	5.231E+05	3.353E+08	839	23
756	951	5.715E+05	4.321E+08	3.267E+11	7.190E+05	5.435E+08	984	33
876	1087	7.674E+05	6.722E+08	5.889E+11	9.522E+05	8.341E+08	1132	45
1002	1224	1.004E+06	1.006E+09	1.008E+12	1.226E+06	1.229E+09	1285	61
1073	1356	1.151E+06	1.235E+09	1.326E+12	1.455E+06	1.561E+09	1369	13
1173	1489	1.376E+06	1.614E+09	1.893E+12	1.747E+06	2.049E+09	1486	-3
1292	1619	1.669E+06	2.157E+09	2.786E+12	2.092E+06	2.703E+09	1623	4
1344	1670	1.806E+06	2.428E+09	3.263E+12	2.244E+06	3.017E+09	1682	12
1378	1721	1.899E+06	2.617E+09	3.606E+12	2.372E+06	3.268E+09	1720	-1
1415	1771	2.002E+06	2.833E+09	4.009E+12	2.506E+06	3.546E+09	1761	-10
1454	1820	2.114E+06	3.074E+09	4.469E+12	2.646E+06	3.848E+09	1804	-16
1496	1873	2.238E+06	3.348E+09	5.009E+12	2.802E+06	4.192E+09	1850	-23
1545	1922	2.387E+06	3.688E+09	5.698E+12	2.969E+06	4.588E+09	1903	-19
1590	1972	2.528E+06	4.020E+09	6.391E+12	3.135E+06	4.985E+09	1952	-20
1635	2019	2.673E+06	4.371E+09	7.146E+12	3.301E+06	5.397E+09	1999	-20
1685	2068	2.839E+06	4.784E+09	8.061E+12	3.485E+06	5.872E+09	2052	-16
1735	2118	3.010E+06	5.223E+09	9.061E+12	3.675E+06	6.376E+09	2104	-14
1769	2169	3.129E+06	5.536E+09	9.793E+12	3.837E+06	6.788E+09	2140	-29
1832	2216	3.356E+06	6.149E+09	1.126E+13	4.060E+06	7.437E+09	2204	-12
1870	2260	3.497E+06	6.539E+09	1.223E+13	4.226E+06	7.903E+09	2243	-17
1913	2306	3.660E+06	7.001E+09	1.339E+13	4.411E+06	8.439E+09	2286	-20
1968	2353	3.873E+06	7.622E+09	1.500E+13	4.631E+06	9.113E+09	2341	-12
1998	2395	3.992E+06	7.976E+09	1.594E+13	4.785E+06	9.561E+09	2370	-25
2048	2439	4.194E+06	8.590E+09	1.759E+13	4.995E+06	1.023E+10	2419	-20
2108	2479	4.444E+06	9.367E+09	1.975E+13	5.226E+06	1.102E+10	2477	-2
2168	2517	4.700E+06	1.019E+10	2.209E+13	5.457E+06	1.183E+10	2534	17
2213	2551	4.897E+06	1.084E+10	2.398E+13	5.645E+06	1.249E+10	2576	25
2318	2582	5.373E+06	1.245E+10	2.887E+13	5.985E+06	1.387E+10	2673	91
45877	55839	7.618E+07	1.363E+11	2.548E+14	9.191E+07	1.634E+11		

Equation of the curve of best fit to data set:
y = -1.080699E-04*x*x + 1.413902*x - 23.34724

Table A22: Cylinder Stress-Strain Data, Companion Cylinder to Beam B2. 3 in. x 6 in. Standard Sulfur-Capped, Paper Molds. Area = 7.07 sq. in.

Load, P, lb.	Stress, psi	Axial Strain, Microstrain Gage 1	Gage 2	Average
0	0	0	0	0
5000	710	-252	-180	-216
10000	1410	-463	-407	-435
15000	2120	-709	-637	-673
21400	3030	-987	-910	-949
25200	3560	-1171	-1115	-1143
30000	4240	-1347	-1405	-1376
36000	5090	-1617	-1845	-1731
40200	5690	-1860	-2181	-2021
41000	5800	-1992	-2250	-2121

APPENDIX B

METHOD OF ANALYSIS OF DATA FOR BEAM SPECIMENS

METHOD OF ANALYSIS OF DATA FOR BEAM SPECIMENS

In 1955, Hognestad, Hanson, and McHenry (23) outlined a criterion for ultimate strength design. Their work was later accepted as a basis for formulating the American Concrete Institute recommendations for ultimate strength design (ACI Standard 318-77).

Their study involved determining the stress block, and the factors K1, K2, and K3 which define it. They also defined stress at a particular fiber as a function of strain, starting from basic assumptions of structural mechanics.

They used a C-shaped structural element similar to the one illustrated in Figure B1.

In the above-mentioned publication, equations defining stress as a function of strain are given as follows:

$$fc = \epsilon \left(df/d\epsilon \right) + f, \text{ and}$$

$$fc = \epsilon \left(dm/d\epsilon \right) + 2m, \text{ where}$$

$$f = \left(P1 + P2 \right) / bc, \text{ and}$$

$$m = \left(P1.a1 + P2.a2 \right) / bc^2.$$

The symbols used above are defined as follows:

fc : concrete compressive stress in extreme fiber of the beam;

ϵ : concrete strain in extreme fiber of beam;

P1 : major thrust;

P2 : minor thrust;

a1 and a2 : lever arms.

(Refer to Figure B1 for physical interpretation of the nomenclature.)

The reinforcement detail is shown in Figures B2 and B3. The loading frame along with location of the hydraulic ram and load cell are shown in Figure B4.

In our investigation to determine the unconfined compressive strength of concrete, we used a specimen (referred to as the beam specimen throughout the body of the text) as illustrated in Figure B1. The method of analysis was that developed by Hognestad, Hanson, and McHenry (21).

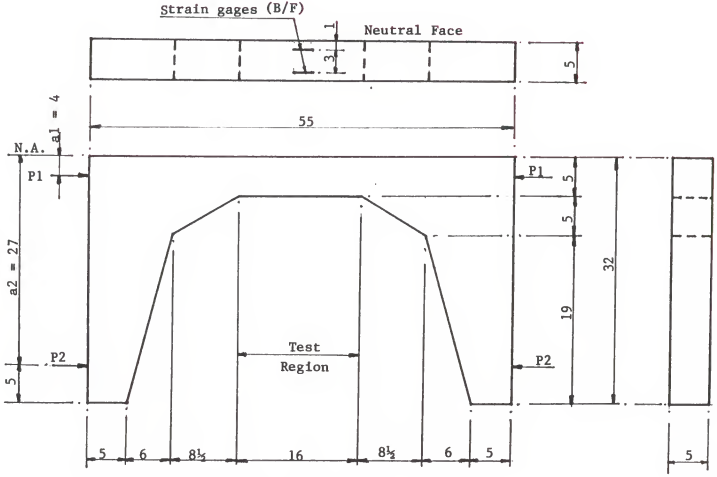

Note: All dimensions are in inches.

Figure B1 : C-Shaped Structural Element (Beam Specimen) used for Determining Unconfined Compressive Strength of Concrete. (Hognestad, McHenry, and Hanson (23)).

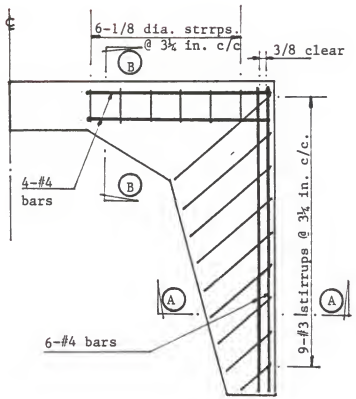

Figure B2 : Plan
(Showing Reinforcement Detail)

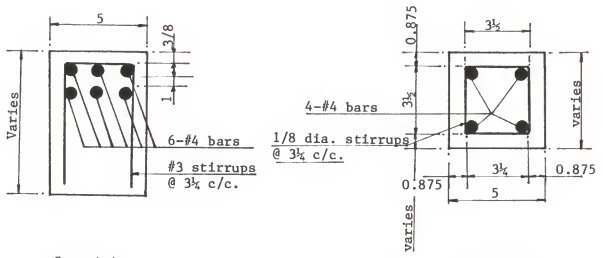

Sec. A-A

Sec. B-B

Figure B3

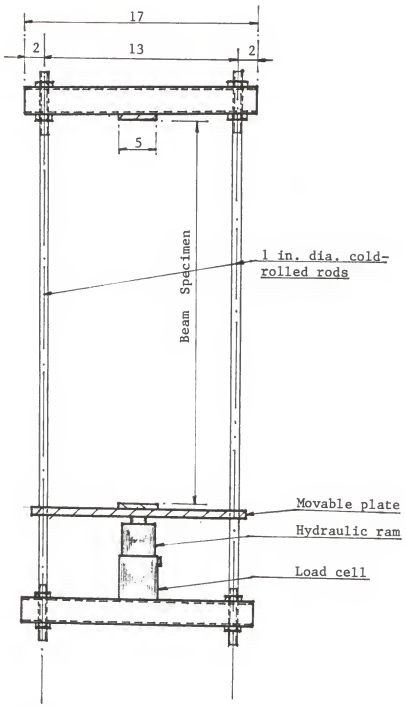

Figure B4 : Loading Frame to apply minor load, P2.

APPENDIX C

BIBLIOGRAPHY

BIBLIOGRAPHY

1. ASTM Annual Book of Standards, current edition.

2. Foeppl, A., "Mitteilungen aus dem Mech.", Tech. Lab. der Koenigs Tech. Hochschule, Munchen, Hefte 27, 1900.

3. Gonnerman, H.F., "Effect of End Condition of Cylinder in Compression Tests of Concrete", Proceedings, American Society for Testing and Materials, Volume 24, Part II, 1924, pp. 1036-1063.

4. Gonnerman, H.F., "Effect of Size and Shape of Test Specimen on Compressive Strength of Concrete", American Society for Testing and Materials, Proceedings, Volume 25, Part II, 1925, pp. 237-250.

5. Troxell, G.E., "The Effect of Capping Methods and End Conditions Before Capping Upon the Compressive Strength of Concrete Test Cylinders", Proceedings, American Society for Testing and Materials, Volume 41, 1941, pp. 1038-1044.

6. Johnson, James W., "Effect of Height of Test Specimens on Compressive Strength of Concrete", Bulletin, American Society for Testing and Materials, Number 120, January, 1943.

7. Tucker, J., "Effect of Length on the Strength of Compression Test Specimens", Proceedings, American Society for Testing and Materials, Volume 45, 1945, pp. 976-984.

8. Mather, B.,"Effect of Type of Test Specimen on Apparent Compressive Strength of Concrete", Proceedings, American Society for Testing and Materials, Volume 45, 1945, 802-809.

9. Price, W.H., "Factors Influencing Concrete Strength", PRoceedings, American Concrete Institute, Volume 47, 1951, pp. 417-432.

10. Neville, A.M., "The Influence of Size of Concrete Test Cubes on Mean Strength and Standard Deviation", Magazine of Concrete Research, London, August, 1956, pp. 101-110.

11. Werner, G., "The Effect of Capping Material on the Compressive Strength of Concrete Cylinders", Proceedings, American Society for Testing and Materials, Volume 58, 1958, pp. 1166-1181.

12. Newman, K., and Lachance, L., "The Testing of Brittle Materials under Uniform Uniaxial Stress", Proceedings, American Society for Testing and Materials, Volume 64, 1964, pp. 1044-1067.

13. Hughes, B.P., and Bahramian, B., "Cube Tests and Uniaxial Compressive Strength of Concrete", Magazine of Concrete Research, Volume 17, Number 53, December, 1965.

14. Kupfer, H., Hilsdorf, Hubert K., and Rusch, Hubert, "Behavior of Concrete Under Biaxial Stresses", American Concrete Institute Journal, Volume 68, Number 8, August, 1969.

15. Seibel, E., and Pomp, A., "Die Ermittlungen der Formanderungsfestigkeit von Matallen durch den Stanchversuch Mitt.", Kaiser-Wilhelm Institute, Eisenforsch, Dusseldorf, Volume 9, 1927, p.157 (as reported by Timoshenko, S., in "Strength of Materials, Part II", O. Van Nostrand and Co., Inc., Princeton, N.J., N.Y., 1958).

16. Schickert, G., "On the Influence of Different Load Application Techniques on the Lateral Strain and Fracture of Concrete Specimens", Cement and Concrete Research, Volume 3, 1973, pp. 487-494.

17. Basunbul, Islam Ahmed, "The Influence of End Friction and Length-to-Diameter Ratio on the Behavior of Concrete Cylinders", Ph.D. Dissertation, University of California, Davis, 1981.

18. Davin, M., "Remarks on the Compression Test with Rubber Caps", International Union of Testing and Research Laboratories for Materials and Structures (RILEM), Bulletin, Number 32, 1956, pp. 49-57.

19. Hansen, H., Nielsen, K.E.C., Kielland, A., and Thaulow, S., "Compressive Strength of Concrete -- Cube or Cylinder", Bulletin, RILEM, Number 17, December, 1962, pp. 23-30.

20. Sigvaldason, O.T., "The Influence of Testing Machine Charecteristics upon the Cube and Cylinder Strength of Concrete", Magazine of Concrete Research, Volume 12, Number 57, December, 1966, pp. 197-206.

21. Mills, Laddie L., and Zimmerman, Roger M., "Compressive Strength of Plain Concrete Under Multiaxial Loading Conditions", American Concrete Institute Journal, Proceedings, Volume 67, Number 10, October, 1970, pp.802-807.

22. Farrar, N.S., "The Influence of Platen Friction on the Fracture of Brittle Materials", Journal of Materials, JMLSA, Volume 6, Number 4, December 1971, pp.889-910.

23. Hognestad, E., Hanson, N.W., and McHenry, D., "Concrete Stress Distribution in Ultimate Strength Design", Journal of the American Concrete Institute, December, 1955, pp. 455-479.

24. Nikaeen, A., "The Production and Structural Behavior of High-Strength Concrete", M.S. Thesis, Kansas State University, 1982.

25. Burmeister, R.A., "Tests of Paper Molds for Concrete Cylinders", Proceedings, American Concrete Institute, Volume 47, 1951, p. 17.

ACKNOWLEDGEMENTS

The author wishes to express his sincere appreciation to Dr. Cecil H. Best, under whose guidance this study was carried out, and to Dr. Stuart E. Swartz and Dr. Albert N. Lin for their helpful criticism.

Sincere thanks are also due to Dr. Robert R. Snell, Dr. James K. Koelliker, Dr. Fredric C. Appl, Messrs. Gary Thornton, Russell L. Gillespie, Brian Holle, Ali Nikaeen, and Ms. Peggy Selvidge. Dr. Snell provided office and laboratory space, equipment, and a portion of the funding. Dr. Koelliker provided instruction and guidance in the use of microcomputers and software. Dr. Appl made his research diamond-tooled lathe available, and Mr. Thornton instructed the author in its use and crafted the steady-rest needed in the facing of longer specimens. Mr. Gillespie taught the author to machine the PVC cylinder molds, to refit elements of the loading yoke for the beam specimens, and to weld the reinforcing bars for the beam specimens. Messrs. Holle and Nikaeen, fellow graduate students, helped the author in experimental work. Ms. Selvidge gave invaluable guidance relative to Graduate School rules and regulations in general, and to thesis requirements in particular.

Major funding for the project was generously provided through grants from Ash Grove Cement, Buildex, and Dudley Williams & Associates, and through contributions to the KSU Foundation from C. H. Best, D. W. Kershaw, Kershaw Ready-Mix Concrete & Sand Company, and Professional Engineering Consultants, P.A.

AN INVESTIGATION INTO THE UNCONFINED COMPRESSIVE STRENGTH OF CONCRETE

by

BISWAJIT MUNSHI

B.E., University of Calcutta, 1978

AN ABSTRACT OF A MASTER'S THESIS

submitted in partial fulfillment of the

requirements for the degree

MASTER OF SCIENCE

Department of Civil Engineering

KANSAS STATE UNIVERSITY
Manhattan, Kansas

1987

ABSTRACT

The standard cylinder test (ASTM C39 : Standard Test Method for Compressive Strength of Cylindrical Concrete Specimens -- Annual Book of ASTM Standards Section 4 - Construction) is used universally to determine the uniaxial compressive strength of concrete.

However, the value of ultimate compressive strength obtained from the standard uniaxial compression test, is, in fact, higher than the true strength of concrete in uniaxial compression.

It is generally believed as a result of the work of several investigators throughout this century that the strength in uniaxial compression of cylindrical test specimens is significantly affected by the end frictional conditions and the geometry of the specimen.

The present investigation was designed to develop a method for determining the strength of concrete in truly unconfined uniaxial compression and to test the method in the context of a design application.

A coincidental part of the investigation was to study lateral and axial deformational charecteristics and other mechanical properties for specimens with different geometries.

Results from this work show that apparently the strength of concrete in truly unconfined compression is in the order of 85 percent of the strength determined from standard cylinders tested in accordance with ASTM C39.